LOW SPEED WIND TUNNEL INVESTIGATION OF HIGH LIFT DEVICES ON A 65° SWEPT-BACK SUPERSONIC WING OF 3.44 ASPECT RATIO

Thesis by

Michael F. Marx

In Partial Fulfillment of the Requirements

For the Degree of

Aeronautical Engineer

California Institute of Technology

Pasadena, California

1949

ACKNOWLEDGEMENT

The author wishes to express his sincere gratitude to Mr. Henry T. Nagamatsu of the GALCIT staff for his advice in conducting the experimental work as well as the preparation of this thesis.

The author further wishes to express his appreciation to Mr. John W. Thomas with whose very able cooperation the experimental work was carried out.

Special thanks go to Dr. E. E. Sechler for his assistance in the design and construction of the model.

TABLE OF CONTENTS

TABLE OF FIGURES

Fig.

SUMMARY

A low speed survey was conducted on a 3.44 aspect ratio wing having a 65° swept-back leading edge and double wedge symmetrical airfoil section to obtain information as to the effectiveness of various high-lift devices. These devices included trailing edge split and extended split flaps, leading edge split flaps, slats and combined configurations. Tests were carried out on the wing with and without the fuselage and horizontal tail surface.

The split flaps increased the lift over the lower ranges of angle of attack only. The extended split flaps increased the lift over the whole angle of attack range. Nose flaps showed practically no gain over any of the range when used by themselves. However, when combined with the trailing edge split flaps in the wing-fuselage configuration, the optimum maximum lift conditions were obtained. Addition of the fuselage and horizontal tail surfaces each produced considerable increments of lift.

In all configurations except leading edge flaps in the inboard position undesirably large negative pitching moments resulted. However, they had stabilizing tendencies except where there were irregularities in the lift curves.

I. INTRODUCTION

With the advent of transonic and supersonic aircraft, there is associated the problem of landing. The wing plan forms as well as airfoil sections of these airplanes by themselves do not produce the necessary lift at low speeds to make landing runs safe or practical. For this reason an experimental investigation was carried out to determine the relative merits of various lift devices on a supersonic wing.

Recently, considerable attention has been focused on this problem. Since the plane is designed to fly at high speeds, the aerodynamicist would like to use the sharp leading edge airfoils and swept wing, both of which lead to structural and low speed performance difficulties. Consequently, some compromise must be made in the design.

Jensen and Koerner (Cf. Ref. 1) investigated a swept-back wing of 65° and a delta wing both having a double wedge symmetrical airfoil. Their general conclusions were that the wings were satisfactory with the proper high lift devices. Lowry and Schneiter (Cf. Ref. 2) tested a wing with 60° sweep-back and a low drag airfoil with results similar to those of Ref. 1.

This report concerns itself with a wing having a higher aspect ratio than those in the reports mentioned above. It was desired to compare results with those of Ref. 1. Therefore, the same wing area, root thickness ratio, sweep-back angle, airfoil section and fuselage were retained. Hence, with the two reports one should be able to determine the effectiveness of lift devices when the wing aspect ratio has been changed. Also, several different high lift devices were tested with the hope of obtaining some which were more effective.

II. DESCRIPTION OF EQUIPMENT AND MODELS

All tests were carried out in the Cal Tech-Merrill wind tunnel which is located at the Pasadena City College, Pasadena, California. This tunnel is a low speed, closed return, rectangular test section type. The maximum speed was about 72.6 M.P.H. which corresponded to a dynamic pressure of about 13.5 pounds per square foot. The model was mounted in the normal attitude on a three-strut support. The balance system was a three-component type which enabled the reading of lift, drag and pitching moment simultaneously. The wing without fuselage was mounted on trunnions at the mean aerodynamic chord and a tail sting. The fuselage was such that it could be clamped to the wing and tail sting.

Wing Model: Details of the model can be seen in Fig. 1. The wing having an area of 0.682 sq. ft. was milled from a piece of solid annealed brass stock. At the center, a solid brass rod was mounted which served as the tail sting. The sweep-back of the leading edge was 65° while that of the quarter chord line from the leading edge was 64°. The wing had a taper ratio of 0.5 and an aspect ratio of 3.44. The root thickness was 4.28% and the tip thickness was 4.55%. The larger tip thickness was due to model fabrication reasons. All chord measurements have been taken in the free stream direction. The twist and dihedral were both zero. The

airfoil section was that of a symmetrical double wedge with the maximum thickness at the 54% chord station.

Fuselage: The fuselage used was one described in Ref. 3 and the details are presented in Fig. 2. The model was split down the centerline so that it could be clamped to the wing and sting. Wing-fuselage fillets were put on with modeling clay after assembly.

Lift devices: All flaps and slats were made from 0.015-inch shim stock which were fastened to the wing with Scotch tape. All flaps were fastened to the lower surface of the wing so as to be on the low velocity side of the wing. In the case of the split flaps, (Cf. Fig. 3), small pieces of modeling clay were placed between the flap and wing to preserve the angle setting.

The horizontal tail surface was that described in Ref. 1. It was made from 0.040-inch dural sheet and could be mounted at two different heights on the vertical tail surface as can be seen in Fig. 9 . This surface had a total area of 18.2 square inches, aspect ratio of 1.50 and leading edge sweep-back angle of 65^{o}. The vertical tail was made from 0.064-inch dural sheet. The area was 10% of the wing area. The aspect ratio was 0.64 and the leading edge sweep-back angle, 65^{o}.

III. DESCRIPTION OF TEST PROGRAM

Although the tunnel could be operated at a maximum dynamic pressure of 13.5 pounds per square foot, the tests were carried out at 8.2 pounds per square foot which corresponded to a Reynolds number of about 244,000 based on the mean aerodynamic chord. The reason for this lower speed was to avoid the vibration in the model rigging which made accurate reading impossible at the higher speeds.

All of the force tests were run from an angle of attack of -4° to 40° by increments of 4° and 2° depending on the regularity of the data. In all cases, the increment was 2° near the stall. Quite often it was necessary to use 2° throughout most of the range to facilitate fairing of the curves.

The trailing edge extended split flap runs on the wing alone were made at deflection angles of 0, 20, 40 and 60 degrees over the complete angle of attack range. Then, in order to approximate better the $C_{L_{max.}}$ vs flap deflection curve, runs were made near the stall at an angle of attack of 10 and 30°. Similar runs were made for the trailing edge split flaps. In both cases of split and extended split flaps, the above runs were carried out with flaps of 40, 70 and 100% span. All the trailing edge flaps were 25% chord.

The tests of 50% span nose flaps of 10 and 20% chord were carried out on the wing alone. Both inboard and outboard positions were tested with flap deflections of 20 and 40°. Also, for the wing alone a 100% nose flap of 10% chord was tested. Again the deflections were 20 and 40°. The final wing alone tests were those of two nose slats having chords of 15 and 23% mean aerodynamic chord measured parallel to the wing centerline.

With the fuselage on the wing the following were tested: 40 and 82% span split and extended flaps with deflections of 0, 20, 40 and 60 degrees; round-nosed nose flap of 50% span, with and without 40% span extended trailing edge flaps.

For the case of the fuselage, tail and wing combination, the following were investigated: no flap condition, extended split flap of 40% span with round-nosed nose flap of 50% span with the horizontal tail in the upper and lower positions.

Photographic tuft studies were made of numerous flap configurations. These studies were made with the tufts taped on the wing. Other studies were made with a long tuft at the end of a probe to gain knowledge of the flow in the regions removed from the wing.

IV. DISCUSSION OF CORRECTIONS

All force and moment coefficients were based on the area and mean aerodynamic chord of the wing alone. The pitching moments were transferred to the mean aerodynamic center which was determined by approximating the trunnion moment vs lift curve by a straight line rather than arbitrarily selecting the slope at zero lift. In this way an aerodynamic center was obtained at 5.7% mean aerodynamic chord. Computing moments about this point gave a pitching moment which varied much less with angle of attack than one taken about an aerodynamic center which was referred to the zero lift region.

At high angles of attack the data may be slightly in error since the wing tips were near the tunnel floor. No corrections were made for this effect since wall corrections for such a highly swept wing were not available.

The model rigging did not allow for model inversion or use of dummy struts so no zero lift corrections were made. Also, the wing alone showed zero lift at an angle of attack of 30' which seemed to agree within experimental error with the 20' flow inclination observed by other investigators using this tunnel.

The only drag correction was a constant strut tare drag coefficient of 0.010 which was subtracted from all values of the drag coefficient. No estimate of strut interference drag was attempted.

V. RESULTS AND DISCUSSION

The results of the force tests are represented in Figs. 12 through 31.

Plain Wing and Wing With Fuselage: Refs. 4 and 5 conclude that a two-dimensional double wedge airfoil such as was selected for this investigation has a $C_{L_{max.}}$ of from 0.7 to 0.8. The swept back wing tested showed a $C_{L_{max.}}$ of 1.18 which was nearly twice that of the two dimensional wing. This fact is not startling when one considers the very high sweep angle and taper ratio of 0.5. The angle of attack for $C_{L_{max.}}$ was reached at 38° for this particular case.

Pitching moment characteristics of the wing alone were quite favorable throughout the whole range of angle of attack when referred to an aerodynamic center at 5.7% M.A.C. from the leading edge. As mentioned before, this point was selected as the aerodynamic center in order to obtain a more nearly constant pitching moment. It may be noted that in determining the aerodynamic center from near the zero lift point results in a location of roughly 36% mean aerodynamic chord which in turn would show the wing to have a notably unstable tendency when the angle of attack is over 5°. Throughout the remaining tests, all pitching moments were computed about the 5.7% M.A.C. point.

The tuft studies shown in Fig. 32 through 37 show that at high angles of attack the wing tips begin to stall. The portion of the wing near the point stalls even at moderately low angles of attack. This seems to indicate slight separation at parts of the sharp leading edge.

The addition of the fuselage to the wing caused an increase in $C_{L_{max.}}$ to 1.3 (Cf. Fig. 13). Moment characteristics were about the same as for the wing alone except that with the fuselage the destabilizing tendency at the stall was not present.

Split Flaps: Generally speaking, the split flaps on the wing without the fuselage were detrimental to $C_{L_{max.}}$. This seems to agree with the results of Ref. 1. Only in the case of the 100% span split flap condition was any gain in $C_{L_{max.}}$ realized, and then only 0.02. The 40 and 70% span configurations all gave lower maximum lift than did the wing alone as indicated in Fig. 15 and 16. Flap angle decreased the maximum lift in all cases except for the 20° deflection of the 100% span flap, where the above gain was observed. However, in the lower ranges of angle of attack, up to about 12°, the split flaps increased the lift with the optimum flap angle of roughly 50°. For the intermediate range, there existed a transition which seemed to indicate a rather radical

change in flow conditions. For the split flaps the moment tendencies were of a stabilizing nature except in the range of transition mentioned above. This result was observed in Refs. 1 and 2.

The results for the wing with split flaps and fuselage are shown in Figs 17 and 18. Here again the peculiar transition range was observed in the moment curves. The overall effects of the flaps with the fuselage on the wing were the same as with the wing without the fuselage. It seems, therefore, that the flow conditions were not radically changed by the fuselage. With the fuselage the optimum flap angle for $C_{L_{max.}}$ was about 40°. At this deflection, the $C_{L_{max.}}$ was 1.34 for the 82% span condition which corresponded to a full flap from the fuselage to the wing tips. For the 40% span flap the maximum lift was lower than that observed with the wing and fuselage alone. Thus, it can be concluded that in the case of the wing with fuselage and split flaps nearly all the gain in maximum lift resulted from the addition of the fuselage and not the flaps. Also in the lower lift ranges, the flaps increased the lift as they did in the case without the fuselage.

Extended Split Flaps: Fig. 5 is a drawing of the extended flaps. They were not called Fowler flaps since they were fastened directly to the wing without any gap.

As shown in Figs 19 through 21, the extended split flaps on the wing without the fuselage gave an increase in lift throughout the angle of attack range. Also, to be observed

is the fact that the optimum flap angle for $C_{L_{max.}}$ was 20°. In all cases, the amount of lift increased with the amount of span covered by the flaps. A test was made at 0° flap deflection in order to determine the effect of flap area addition alone. The result showed that flap deflection increased $C_{L_{max.}}$ 0.04 over that of the 0° deflection state.

As with the split flaps, the extended split flaps showed increase in lift with flap angle in the lower lift ranges but in the neighborhood of 20° angle of attack the transition range again occurred. As with the split flaps, the transition in lift was accompanied by an unstable tendency as shown by the pitching moment curves. As could be expected, the addition of the extended split flaps resulted in large negative pitching moments which were as large as -.55 for the 100% span flap at a deflection of 40°. It is questionable whether so large a moment could be overcome with permissible tail length and surface.

From the veiwpoint of increasing the maximum lift, one can safely say that the extended split flaps are much more effective than the split flaps, producing at times, an increment in $C_{L_{max.}}$ of 0.46 (Cf. Figs. 14 and 19).

Nose Flaps and Slats: In order to improve the flow over the wing by preventing the early separation at the leading edge as a result of its sharpness, it was decided to try various ramifications of nose flaps and slats. These are shown in Figs. 7 and 8.

Figs. 24 through 27 show, without exception, that the maximum lift was increased by these leading edge lift devices. The maximum lift coefficient reached here was 1.4, obtained through the use of the 50% nose flap in the inboard position. Probably a more important result than this increase in lift in the upper ranges only is the fact that the lift curve no longer has the transition region observed with the flaps in the trailing edge position. This seems to indicate that there has been some improvement in the flow conditions which may make the trailing edge flaps more effective in the upper ranges where before they experienced a decrease in lift rate. The nose slat showed practically no change in wing characteristics when used by itself. For this reason no further tests were carried out on it.

Coming back to the nose flaps, Figs. 25 and 26 show the expected result on the pitching moment when the flaps are placed in the inboard and outboard positions. Placing the flaps inboard gives the wing unstable tendencies but at the same time gives a slightly greater increment in maximum lift than when in the outboard position.

The round-nosed nose flap shown in Fig. 11 when used by itself increased the maximum lift coefficient by 0.02

while in the lower ranges the lift was slightly decreased (Cf. Fig. 30). But as with the nose flaps, the lift curve was fairly regular and the moment stabilizing, even if large at high lift.

The addition of the fuselage, 40% span trailing edge extended flaps and round-nosed nose flaps, (Cf. Fig. 30), produced a maximum lift coefficient of 1.60. The wing and fuselage curves of Fig. 13 showed 1.30. Nose flaps increased this figure to 1.32 when used without the trailing edge flaps. This shows a gain of 0.02 (Cf. Fig. 30). The extended trailing edge flaps in Fig. 21 showed a gain of 0.22. This means that by using the combined configuration the increment in $C_{L_{max.}}$ of 0.06 was added to the sum obtained by using the nose and trailing edge flaps separately. In addition, the magnitude of the pitching moment is of the same order as for the trailing edge flap alone but now has stable characteristics throughout nearly the whole angle of attack as indicated in Fig. 30.

Miscellaneous Configurations: Referring to Fig. 31, the effect of the horizontal tail surface was to increase the maximum lift coefficient by 0.12 when the wing and fuselage with no high lift devices were tested. For this same case the maximum negative pitching moment coefficient was increased about 150%. Stable tendencies were present through the complete range.

The combination of wing with leading edge round-nosed nose flap, the trailing edge extended flap, fuselage and horizontal tail gave the maximum lift coefficient of 1.8 which shows an increase of 0.62 over that obtained from the wing alone. The moment curve shows definite stable tendencies over the whole range with a maximum moment of - .70 (Cf. Fig. 31). It is noteworthy that the definite transition region witnessed when the wing was tested with trailing edge devices alone was decreased, if not eliminated, by the addition of the nose flaps. The pitching moment is very large when these configurations are used but stable tendencies are evident.

Flow Conditions: In order to investigate the transition region which was encountered with the use of the trailing edge flaps, it was decided to conduct a tuft study of the wing especially in those regions where the lift and moment curves were most irregular.

Considering the curves (Cf. Fig. 15) for the wing with the 70% span split flap set at a deflection of 20° one can see the irregularities in the lift curve which are accompanied by corresponding irregularities in the moment curve. Fig. 32 shows the tufts corresponding to an angle of attack of zero degrees. Fig. 33 is the same configuration only at 8° angle of attack. Slightly aft of the tip, one tuft has begun to fluctuate rather violently while at the

midspan position, the tufts are stationary but starting to slant outboard from the wing centerline. None of these indications were evident at zero degrees. Fig. 35 shows conditions at 16° angle of attack. Here the tufts are following the pattern indicated at 8° only in a much more exaggerated manner. Outside of the region near the tip, there still is no oscillation of the tufts. Yet, they are being inclined more and more. By this time the lift and moment curves show definite changes in force characteristics. Figs. 36 and 37 show the wing at an angle of attack of 20° and 24° respectively. Up to this period the wing has not stalled in the usual sense. However, there is turbulent flow at the leading edge near the point of the wing. This seems to indicate that there might be separation from the sharp leading edge.

A survey of the region adjacent to the wing with a long tuft fastened to the end of a probe seemed to indicate that at each side of the centerline of the wing a large vortex was shed which seemed to start at the separation point at the leading edge shown by the contact tufts. This vortex built up in size as it passed downstream, reaching the area about 4 inches above the wing in some cases.

Examination of Fig. 39 shows the same separation starting at the leading edge near the tip for the plain wing.

The subsequent pictures show flow bent away from the sting. This means that the two vortices are shed even by the plain wing. Here the effects on the force curves are not as pronounced as they were with the flapped wing.

VII. CONCLUSIONS

From this investigation fora 3.44 aspect ratio, tapered, highly swept-back supersonic wing the following conclusions may be drawn:

1. The maximum lift coefficient of the swept-back wing was about 65% higher and occurred at a much higher angle of attack than for a two-dimensional wing having the same airfoil characteristics.

2. Split flaps by themselves were detrimental to maximum lift coefficient but increased the lift in the lower ranges. Optimum flap setting for the wing alone was 20° and for the fuselage, 40°.

3. Extended split flaps increased lift over the whole range of angle of attack. For the lower ranges, the optimum flap angle for lift was over 60°, the maximum angle tested. For the maximum lift, the optimum angle was 20°.

4. The effect of the nose flaps was to increase lift at the higher ranges but not at low angles of attack. The general influence of the nose flaps was to decrease the effect of the transition range in the lift curve.

5. The maximum lift coefficient of 1.78 was obtained with the combination of the round-nosed nose flap, 40% extended split flap, fuselage and horizontal tail surface.

6. Below stall, moments were of a stable nature for all trailing edge combinations tested, except where there were irregularities in the lift curve.

7. The effect of adding the fuselage to the wing was to increase the slope of the lift curves and improve stability.

8. The horizontal tail improved stability and added to the maximum lift.

REFERENCES

1. Jensen, A.J., and Koerner, W.G.: Wind Tunnel Investigation of a Supersonic Tailless Airplane At Low Subsonic Speed. Thesis, California Institute of Technology (1948)

2. Lowry, J.G. and Schneiter, L.E.: Investigation At Low Speed of the Longitudinal Stability Characteristics of a 60° Swept-Back Tapered Low-Drag Wing. N.A.C.A.T.N. No. 1284 (May, 1947)

3. Dore, Frank: The Design of Tailless Airplanes. Thesis, California Institute of Technology (1947)

4. Pollock, A.D., Jr. and Reck, F.F.: A Study of Methods to Increase the Lift of Supersonic Airfoils at Low Speed. Thesis, California Institute of Technology. (1947)

5. Hilton, W.F. and Pruden, F.W.: Subsonic and Supersonic High Speed Tunnel Tests of a Faired Double Wedge Aerofoil. R. & M. No. 2057 (Dec., 1943)

FIG. 1

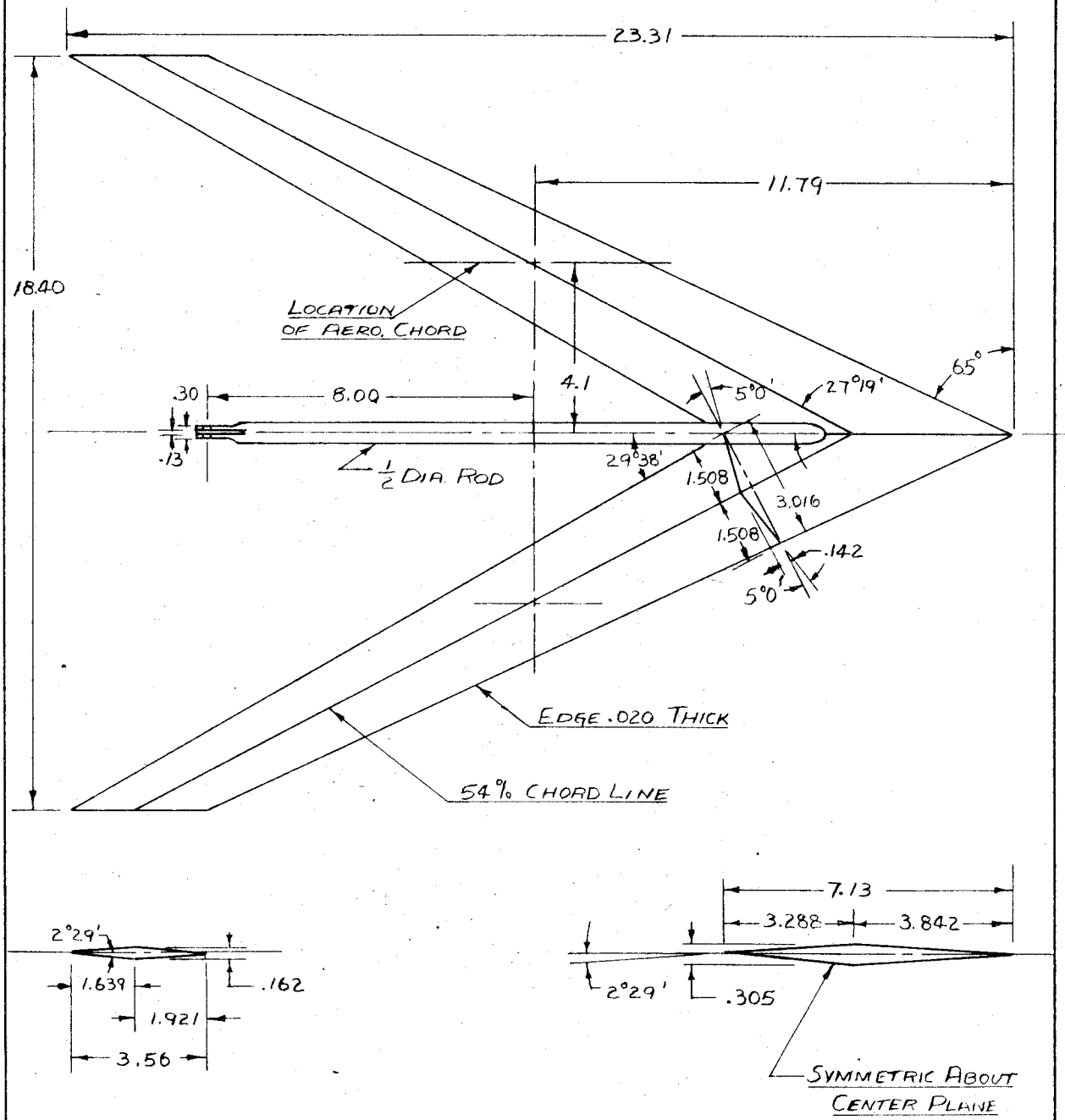

SWEPT BACK WING

AREA: 98.3 SQ. IN.
ASPECT RATIO: 3.44
SPAN: 18.4 IN.
ROOT THK'S: 4.28 %
TIP THK'S: 4.55 %
M.A.C.: 5.54"
SWEEPBACK L.E.: 65°
SWEEPBACK ¼ CHORD LINE: 64°
TAPER RATIO: .5

FIG. 2

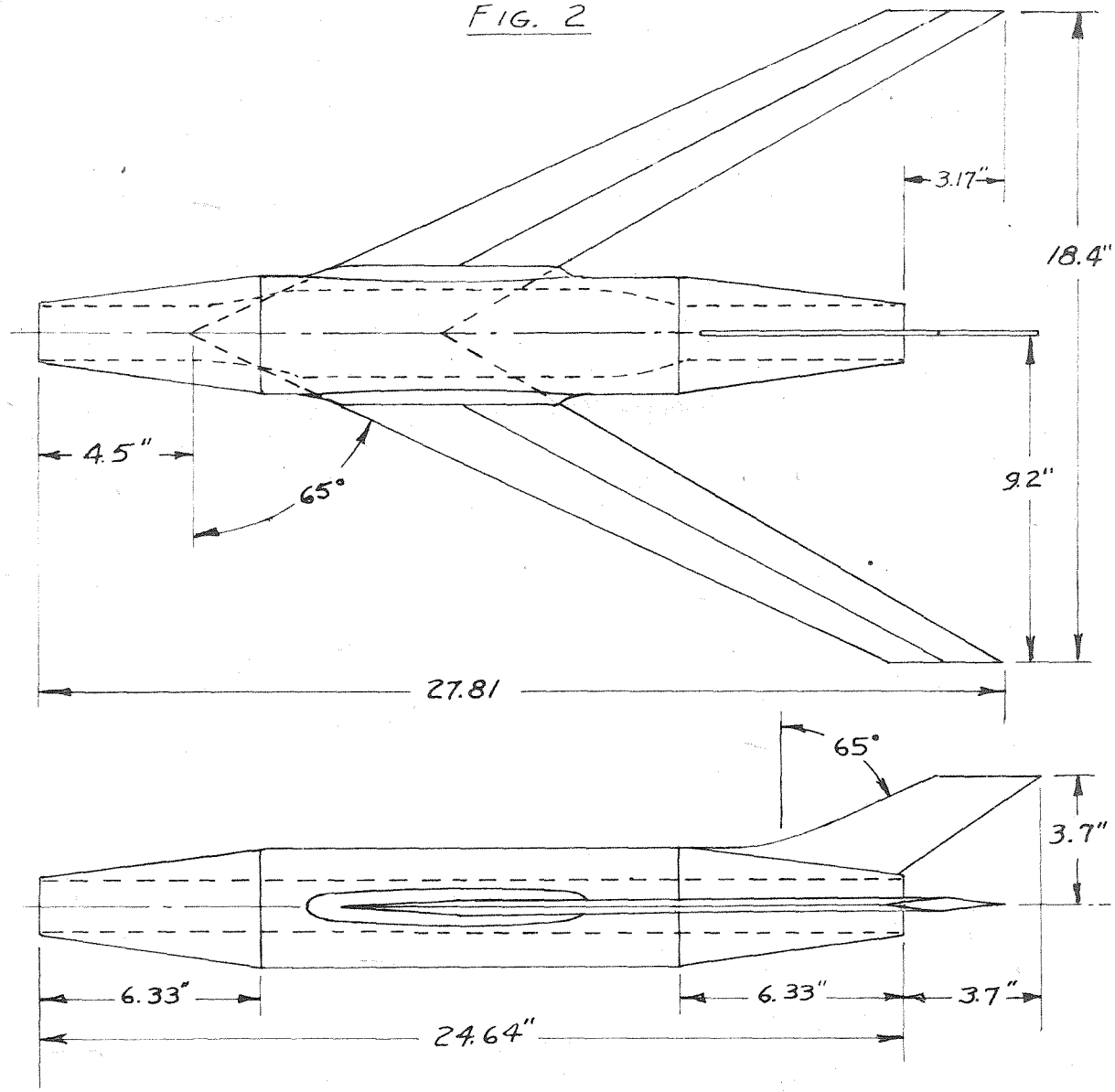

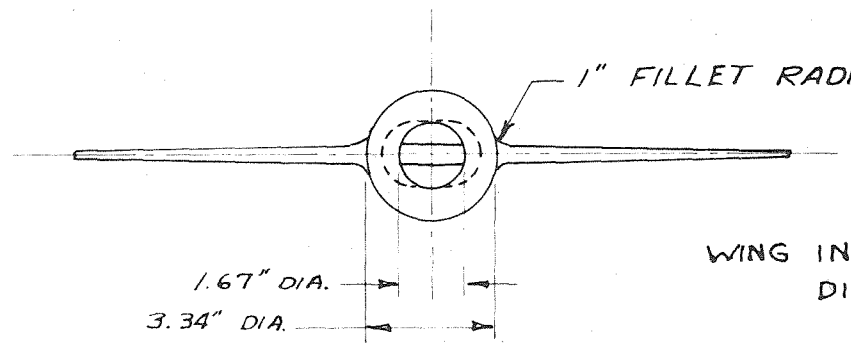

WING INCIDENCE: 0°
DIHEDRAL : 0°

SWEPT-BACK WING WITH FUSELAGE

FIG. 3

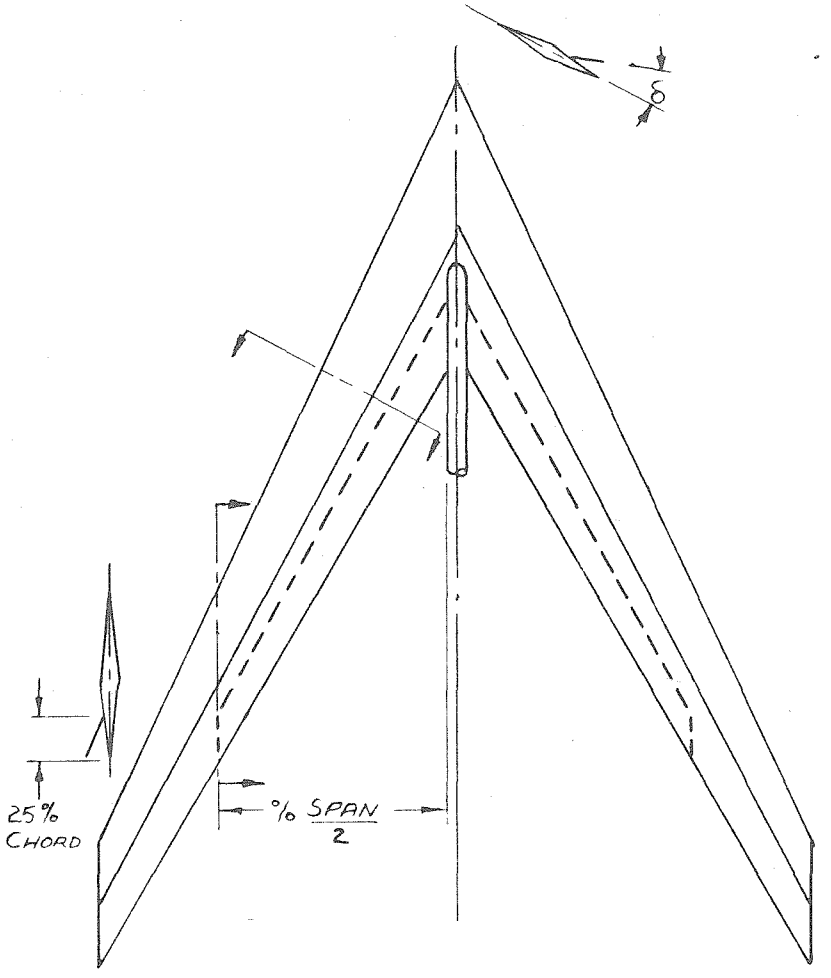

SWEPT BACK WING WITH
SPLIT FLAPS

SPAN	% WING AREA
40	10
70	17.5
100	24.3

FIG. 4

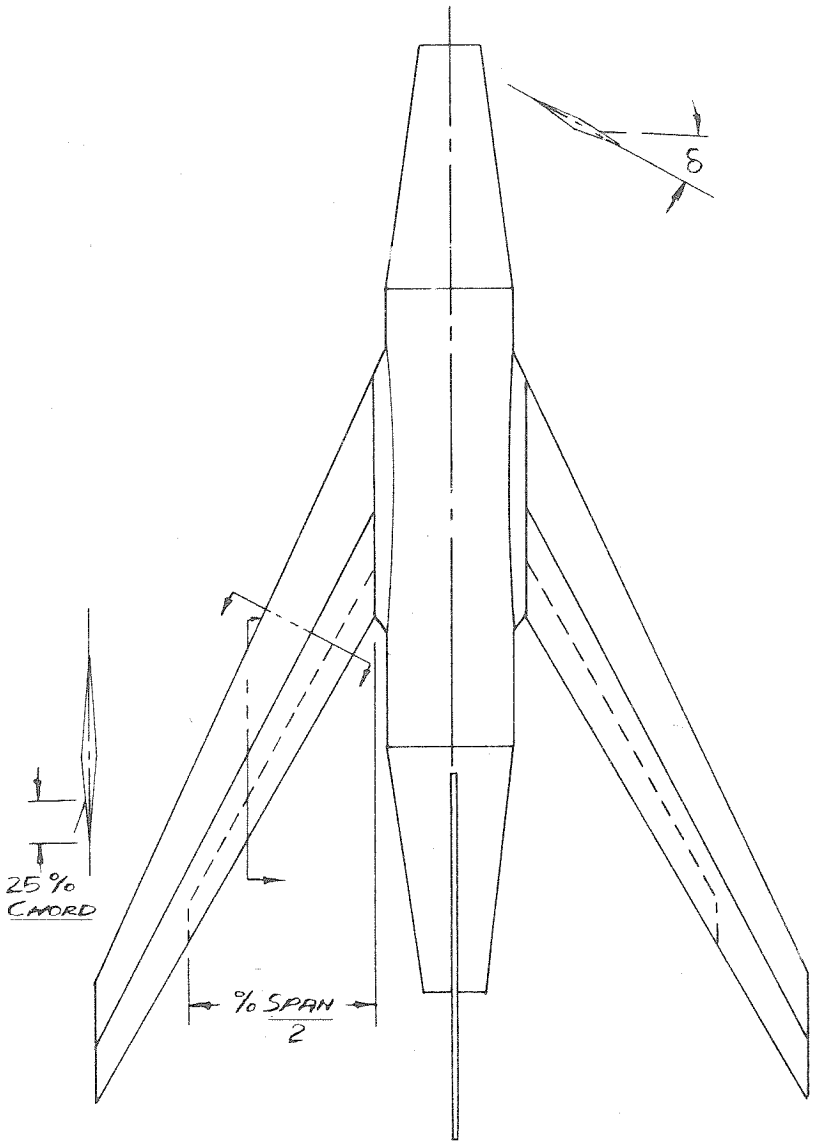

SWEPT BACK WING WITH FUSELAGE AND SPLIT FLAPS

SPAN	% WING AREA
40	10
82	20.5

FIG. 5

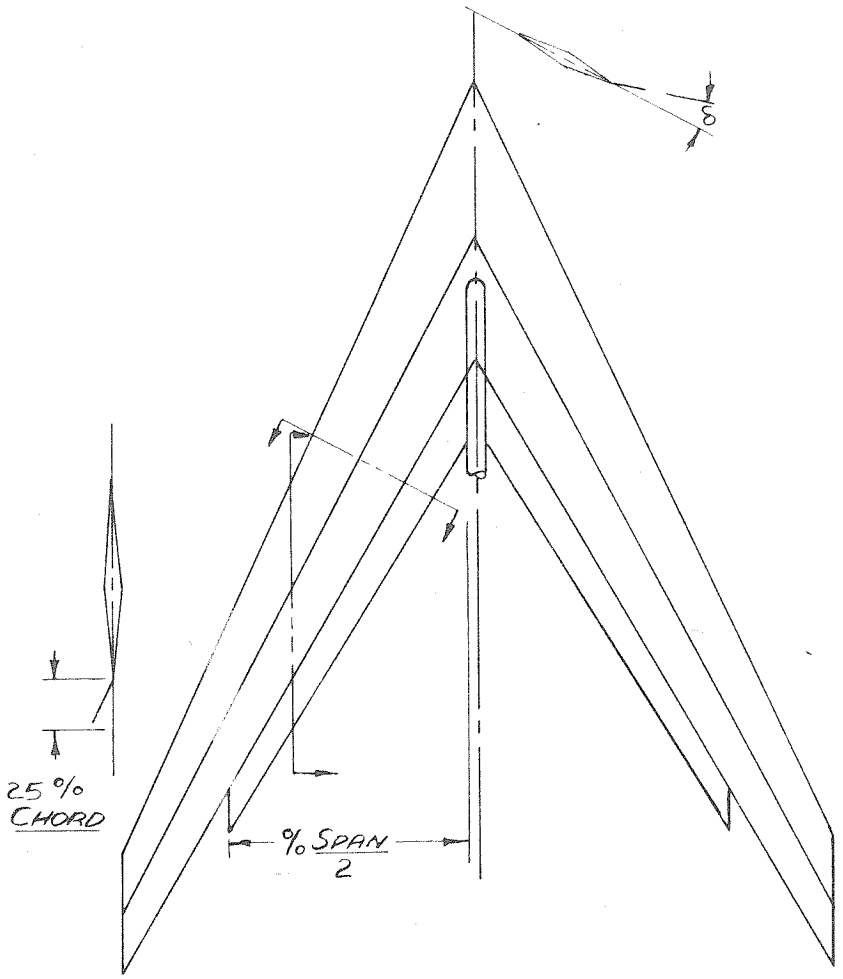

SWEPT BACK - WING WITH
EXTENDED SPLIT FLAPS

SPAN	% WING AREA
40	10
70	17.5
100	24.3

FIG. 6

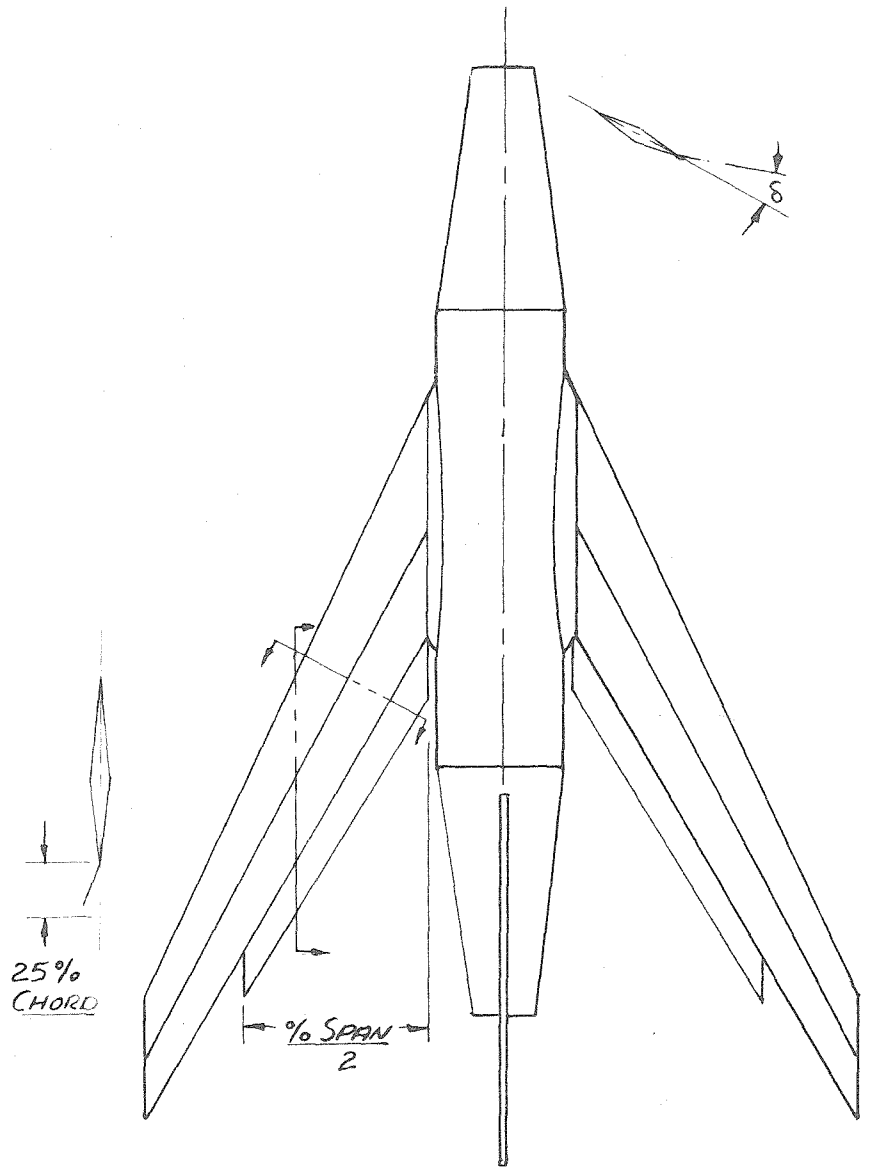

SWEPT BACK WING WITH FUSELAGE
AND EXTENDED SPLIT FLAPS

% SPAN	% WING AREA
40	10
82	20.5

FIG. 7

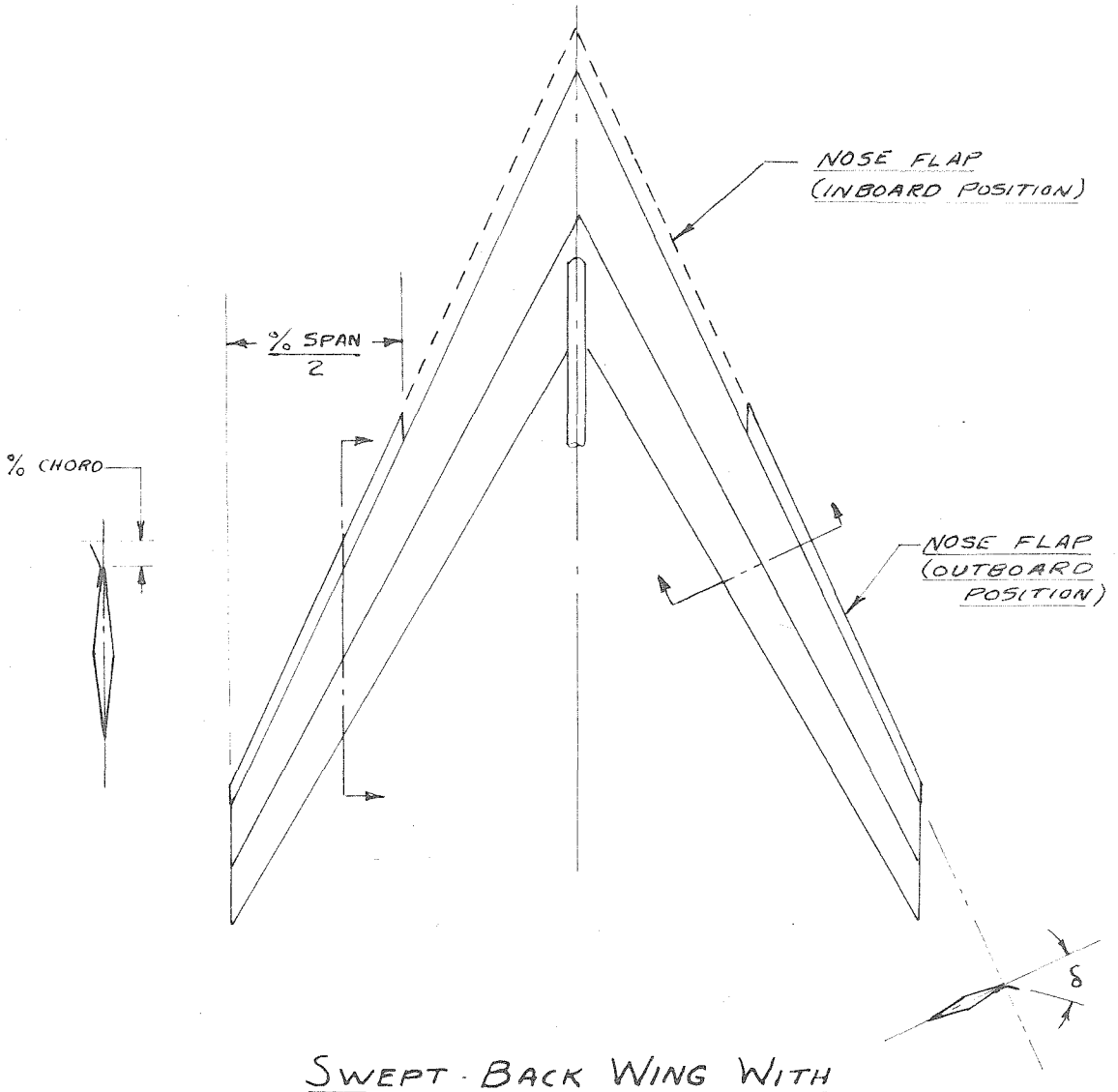

SWEPT-BACK WING WITH NOSE FLAPS

% SPAN	% CHORD	% WING AREA
50	10	5
50	20	10
100	10	10

FIG. 8

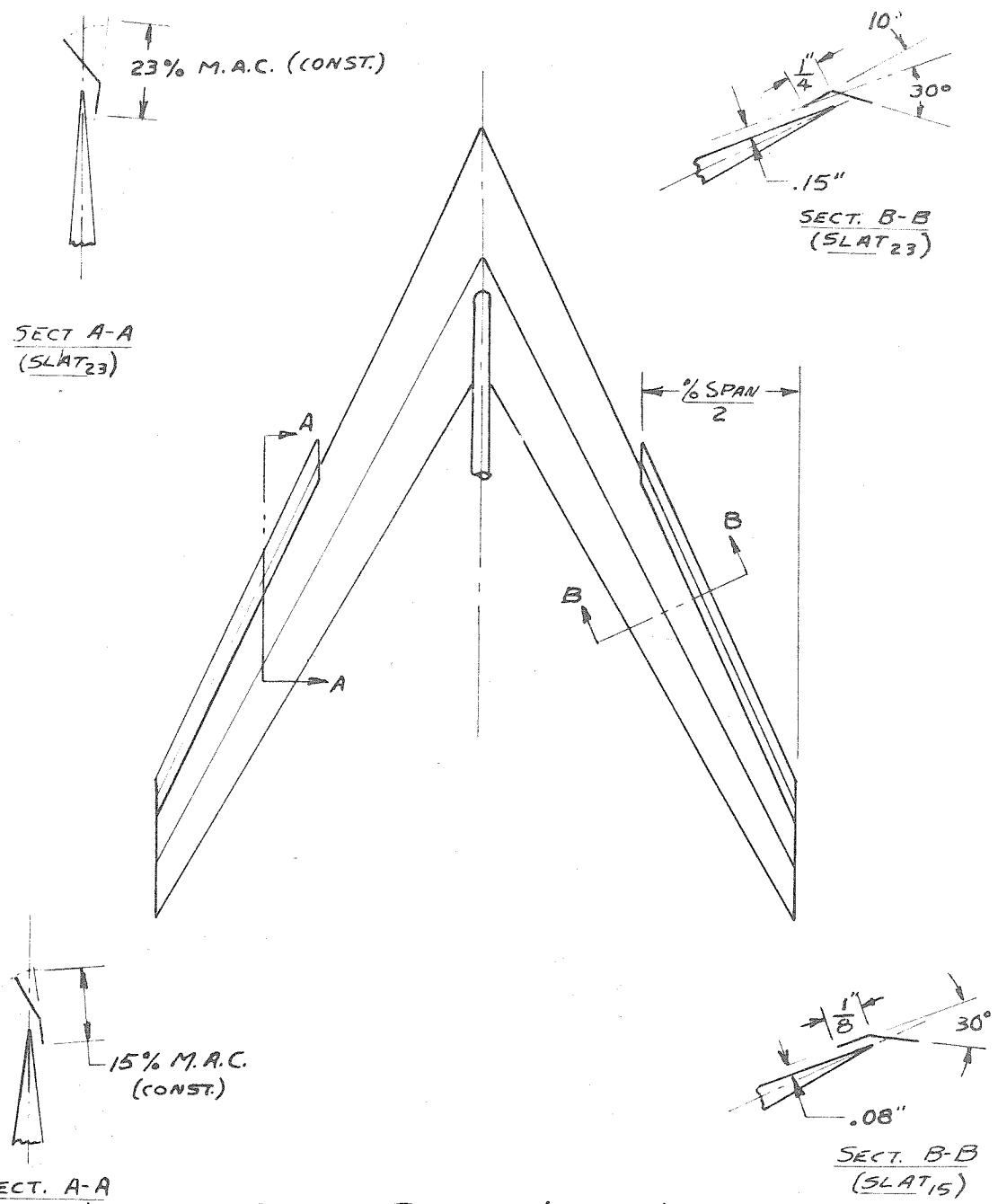

SWEPT-BACK WING WITH NOSE SLATS

% SPAN	% M.A.C.	% WING AREA
50	15	7.8
50	23	11.9

FIG. 9

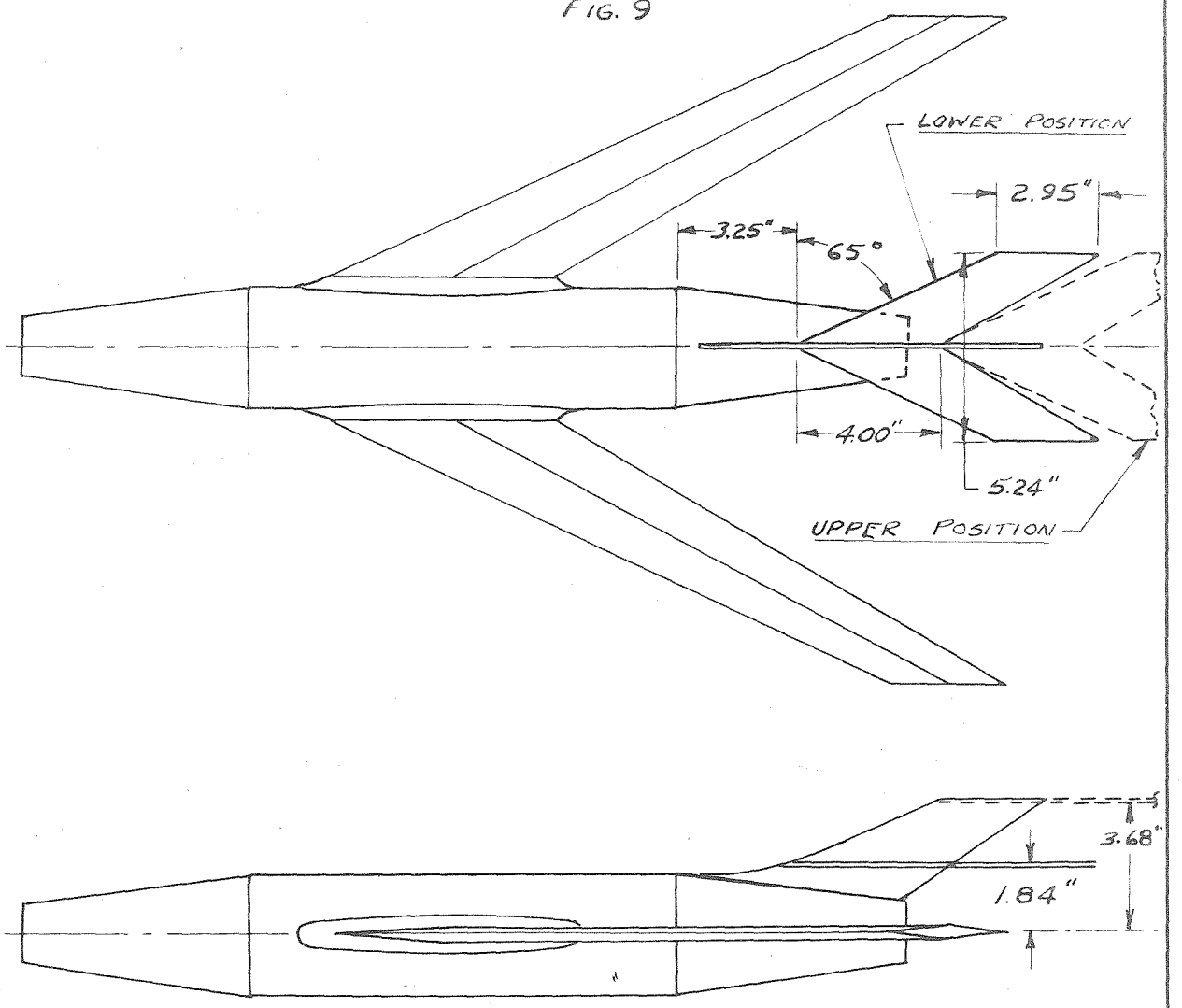

SWEPT-BACK WING WITH FUSELAGE
AND HORIZONTAL TAIL SURFACE

HORIZONTAL TAIL SURFACE:
AREA: 18.5% OF WING AREA
ASPECT RATIO: 1.5

FIG. 10

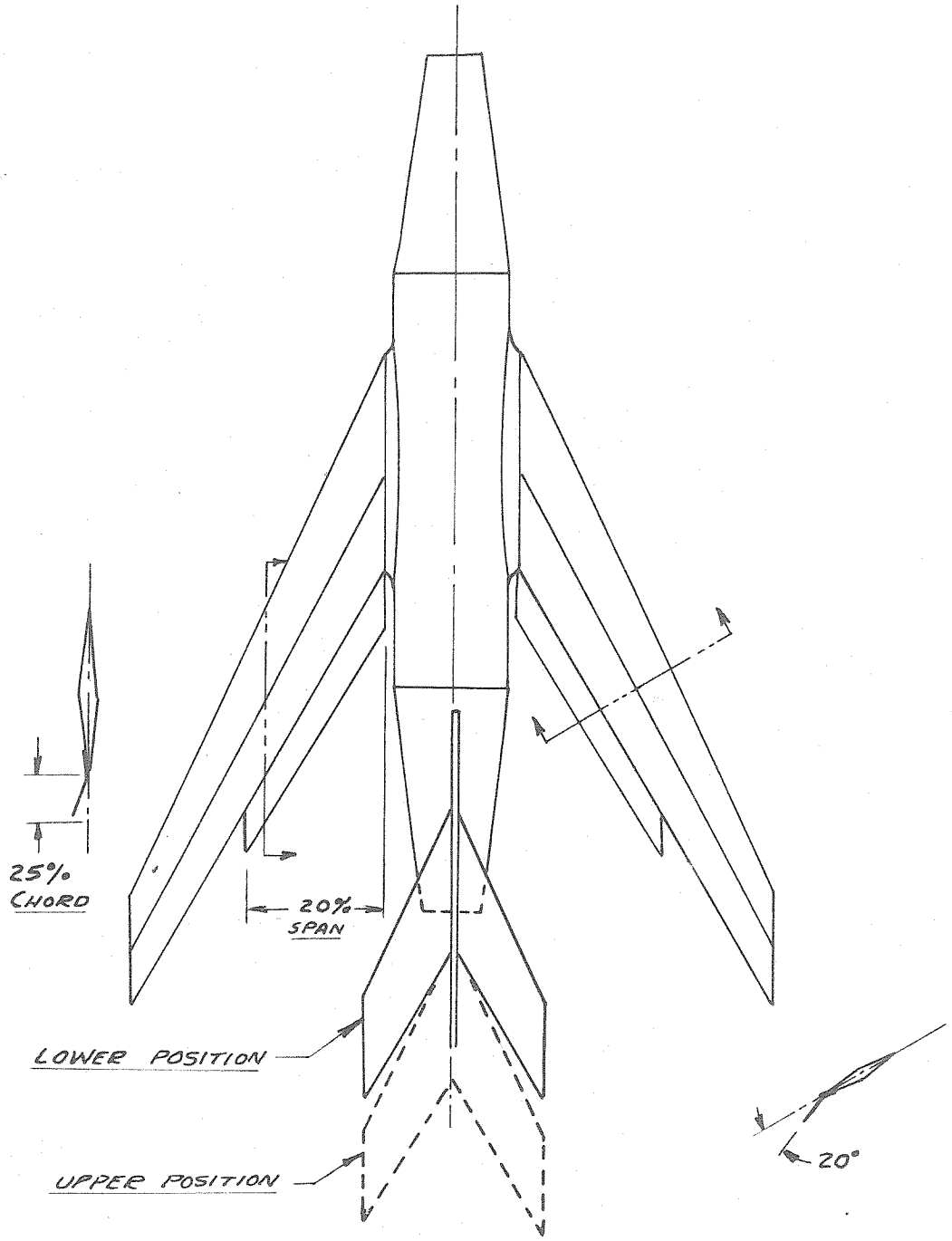

SWEPT-BACK WING WITH FUSELAGE,
HORIZONTAL TAIL SURFACE, AND
40% SPAN EXTENDED SPLIT FLAP

	% OF WING AREA
HORIZONTAL TAIL SURFACE:	10
40% SPAN FLAP	18.5

FIG. 11

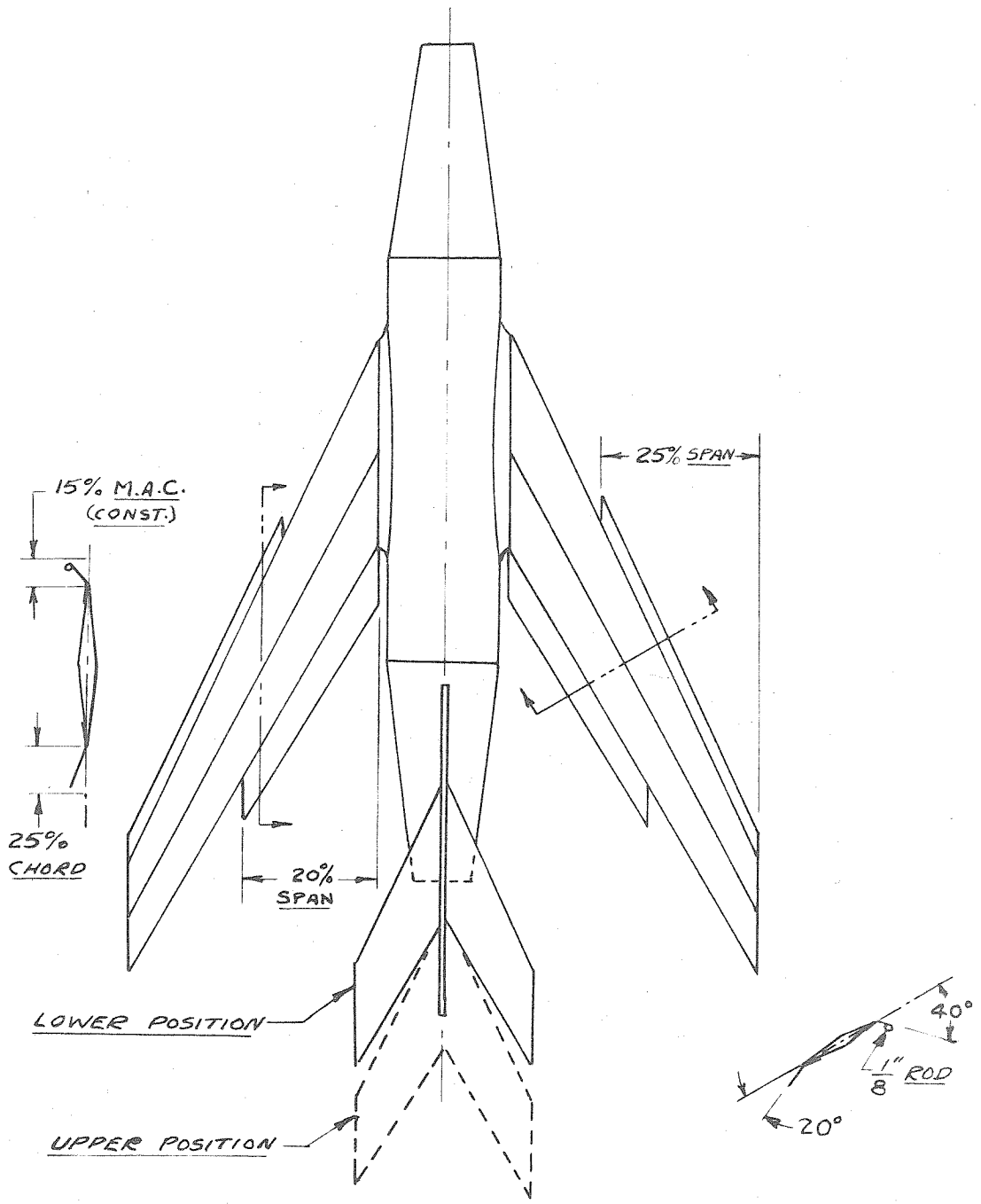

SWEPT-BACK WING WITH FUSELAGE, HORIZONTAL TAIL SURFACE, 40% SPAN EXTENDED SPLIT FLAP, AND 50% SPAN ROUND-NOSED NOSE FLAP

	% OF WING AREA
HORIZONTAL TAIL SURFACE:	18.5
40% SPAN EXTENDED SPLIT FLAP:	10
50% SPAN ROUND-NOSED NOSE FLAP:	7.8

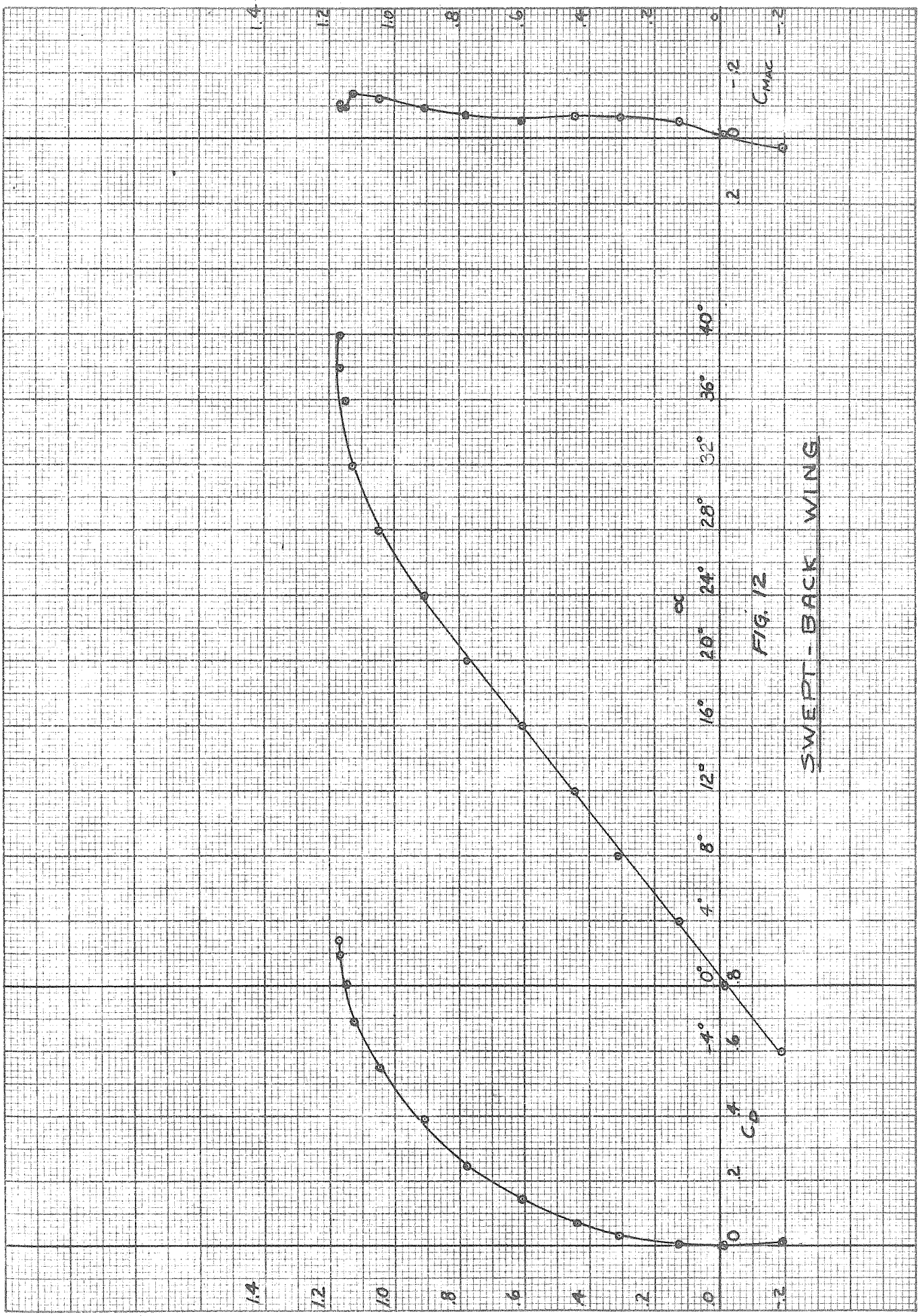

FIG. 12

SWEPT - BACK WING

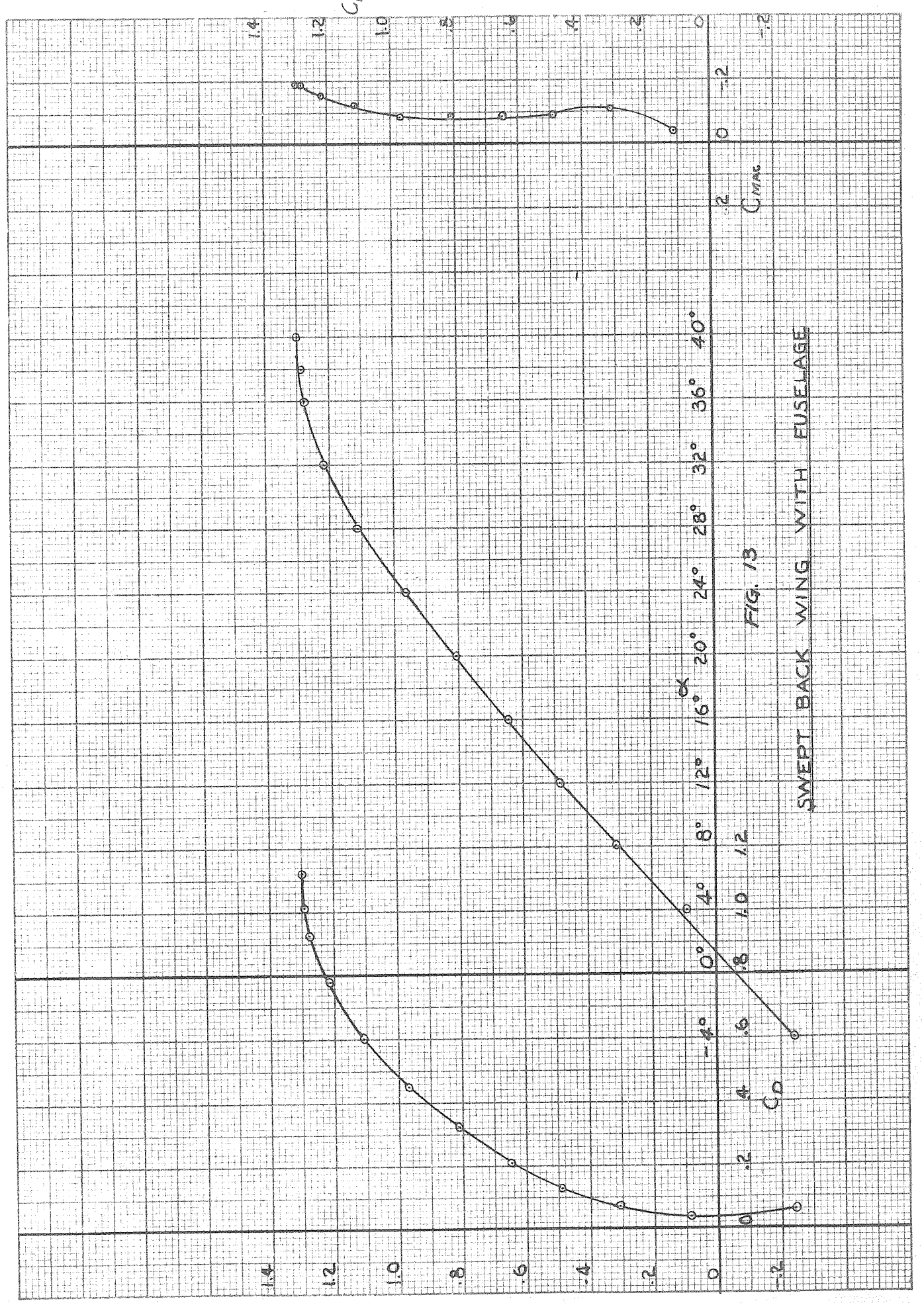

FIG. 13

SWEPT BACK WING WITH FUSELAGE

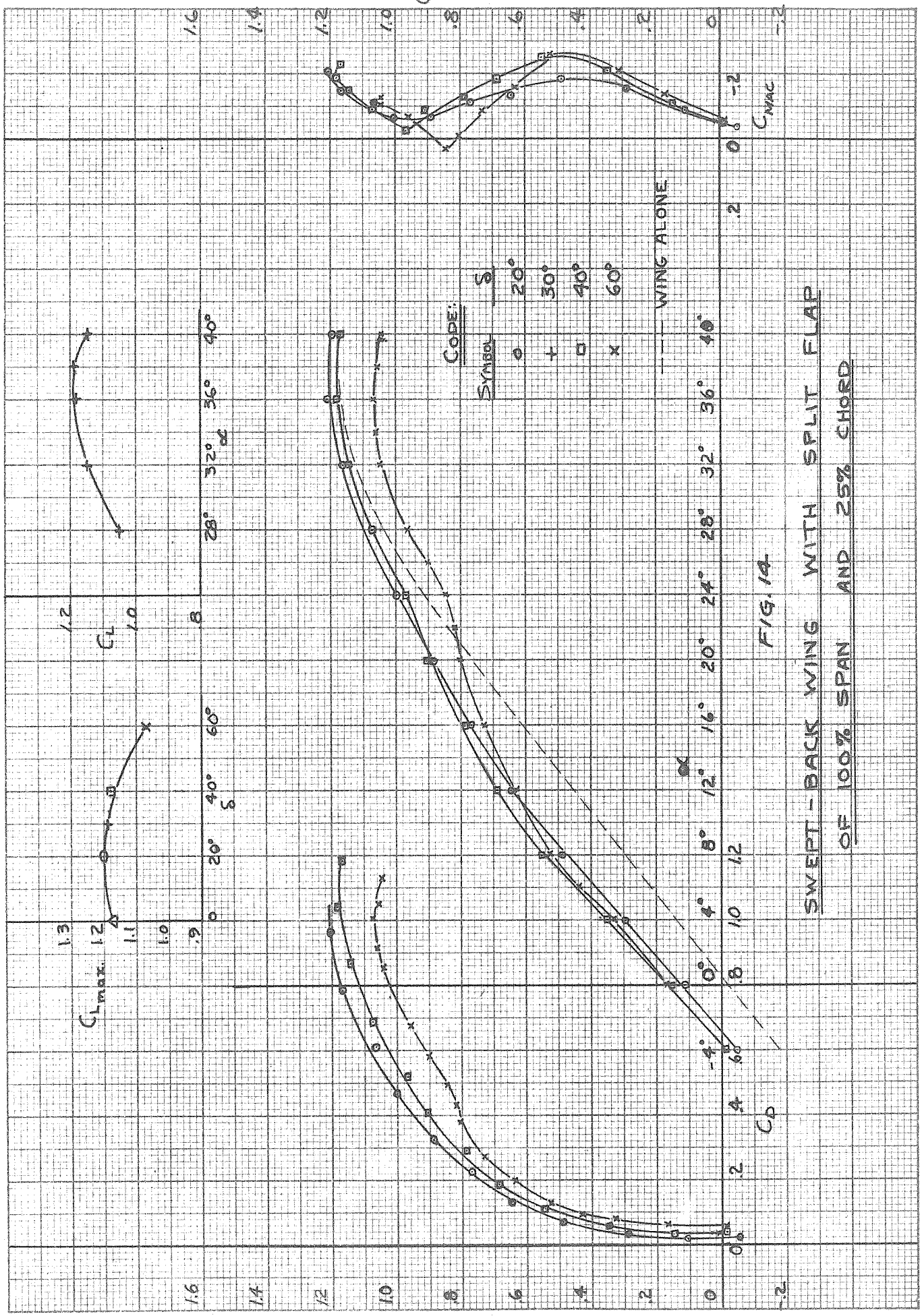

FIG. 14

SWEPT-BACK WING WITH SPLIT FLAP
OF 100% SPAN AND 25% CHORD

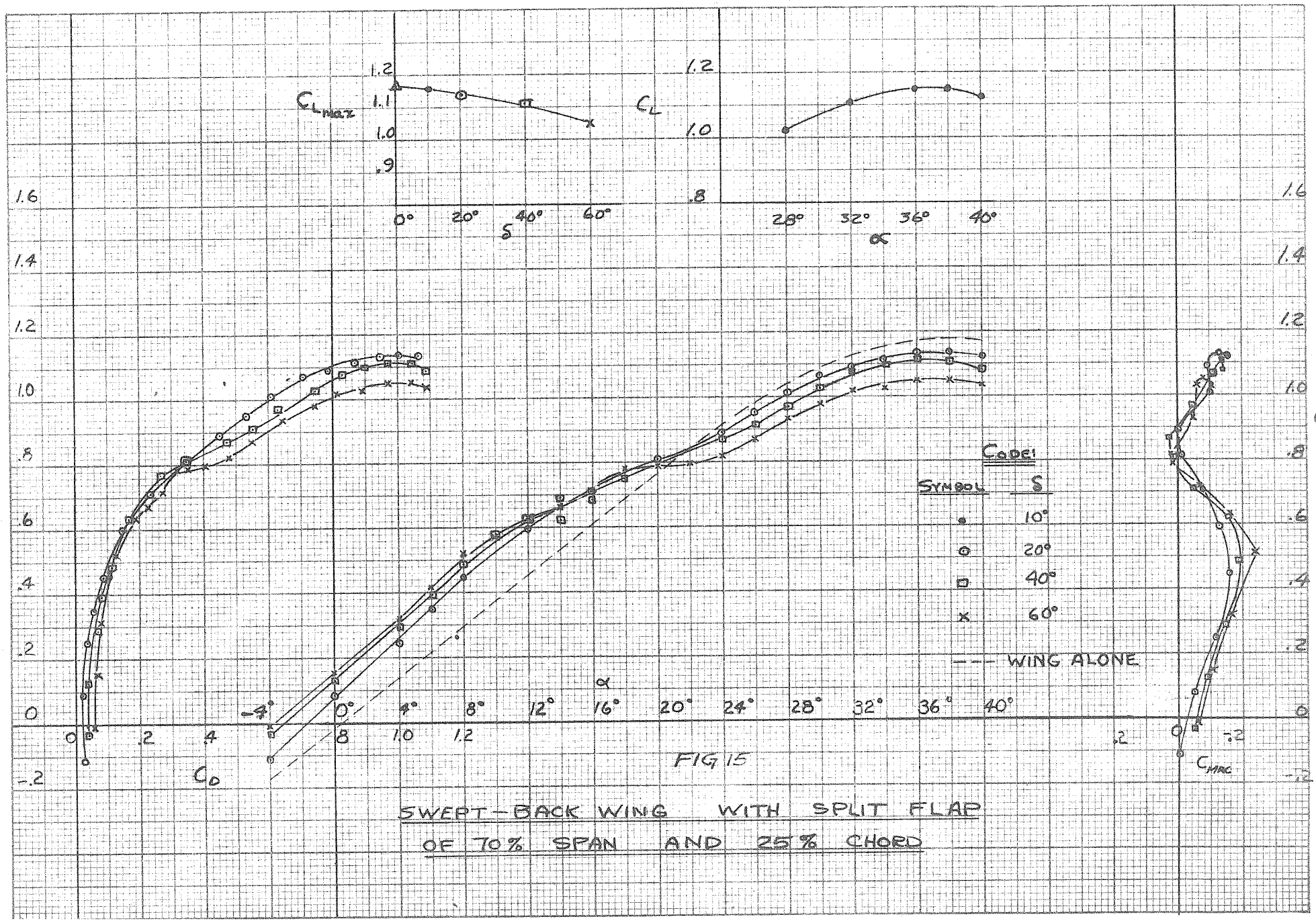

FIG 15

SWEPT-BACK WING WITH SPLIT FLAP
OF 70% SPAN AND 25% CHORD

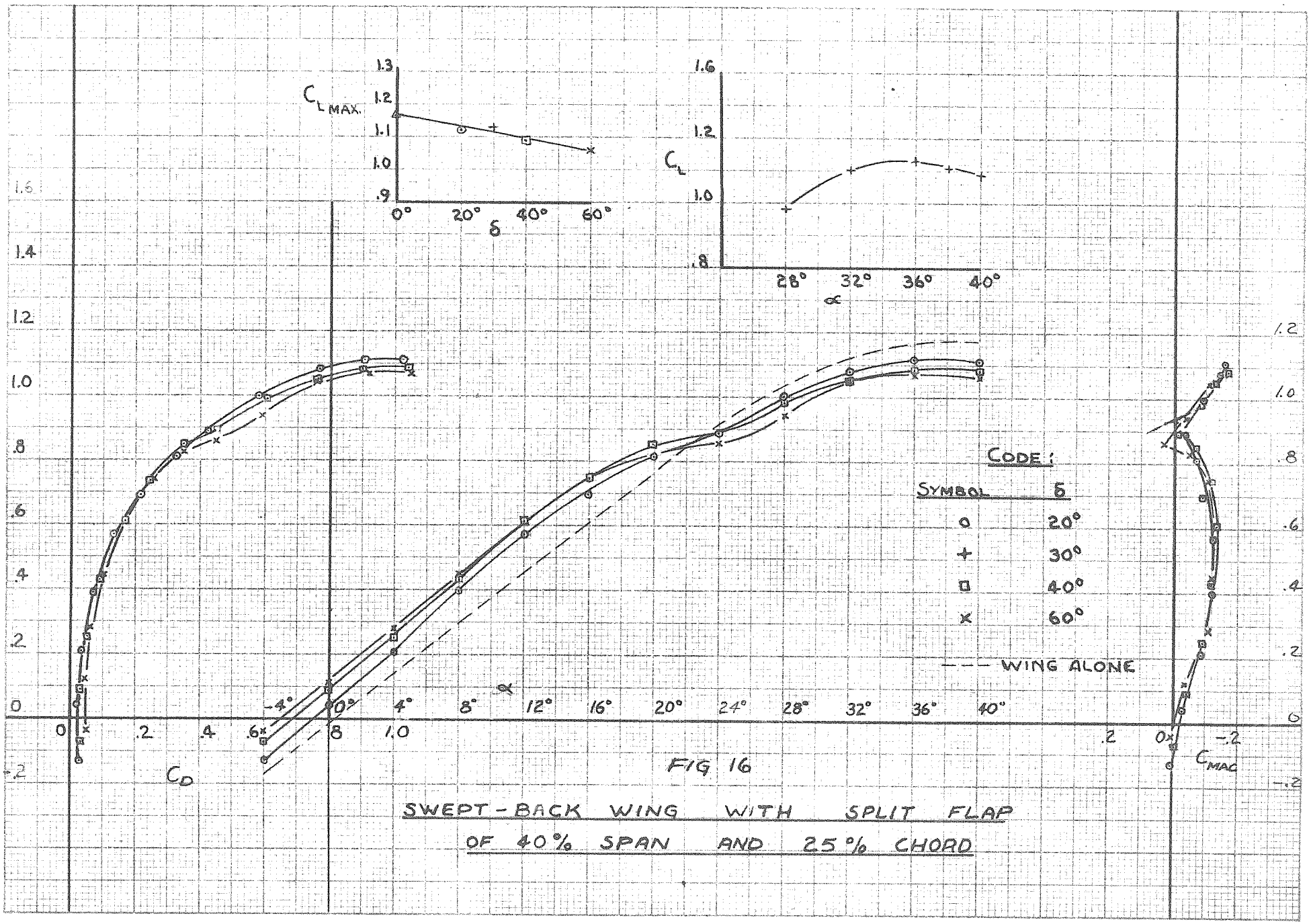

FIG 16

SWEPT-BACK WING WITH SPLIT FLAP
OF 40% SPAN AND 25% CHORD

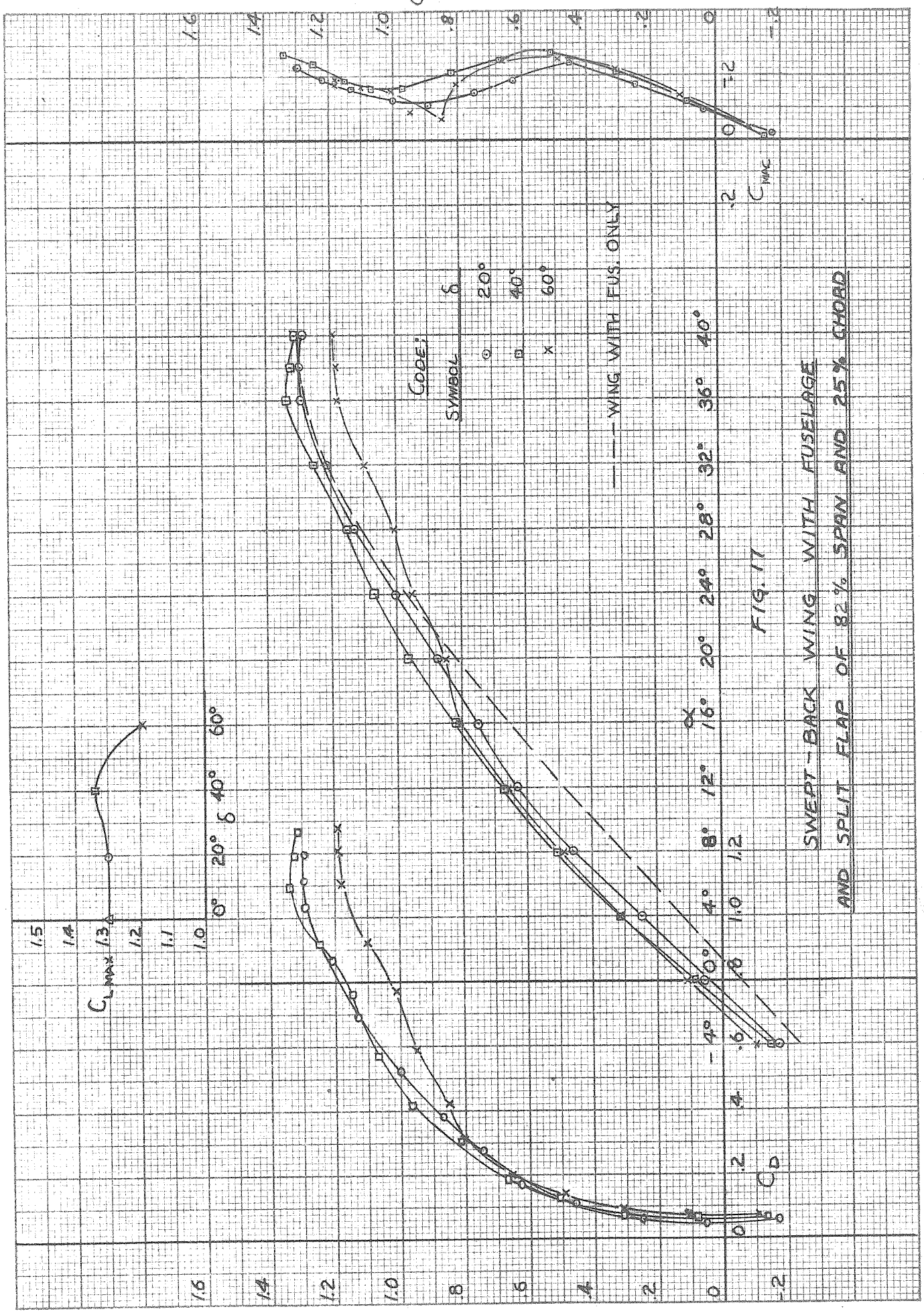

FIG. 17

SWEPT-BACK WING WITH FUSELAGE AND SPLIT FLAP OF 82% SPAN AND 25% CHORD

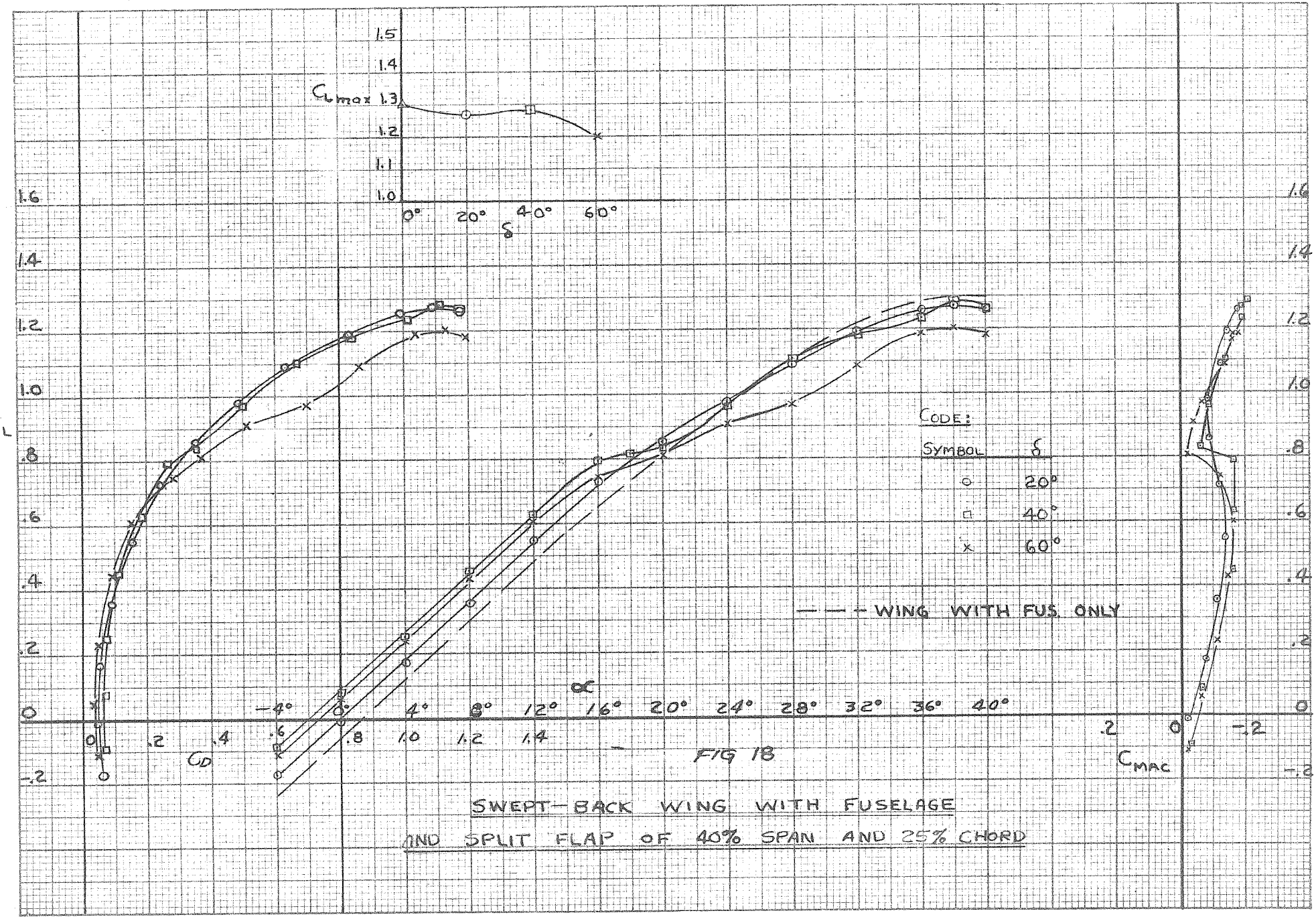

FIG 18

SWEPT-BACK WING WITH FUSELAGE AND SPLIT FLAP OF 40% SPAN AND 25% CHORD

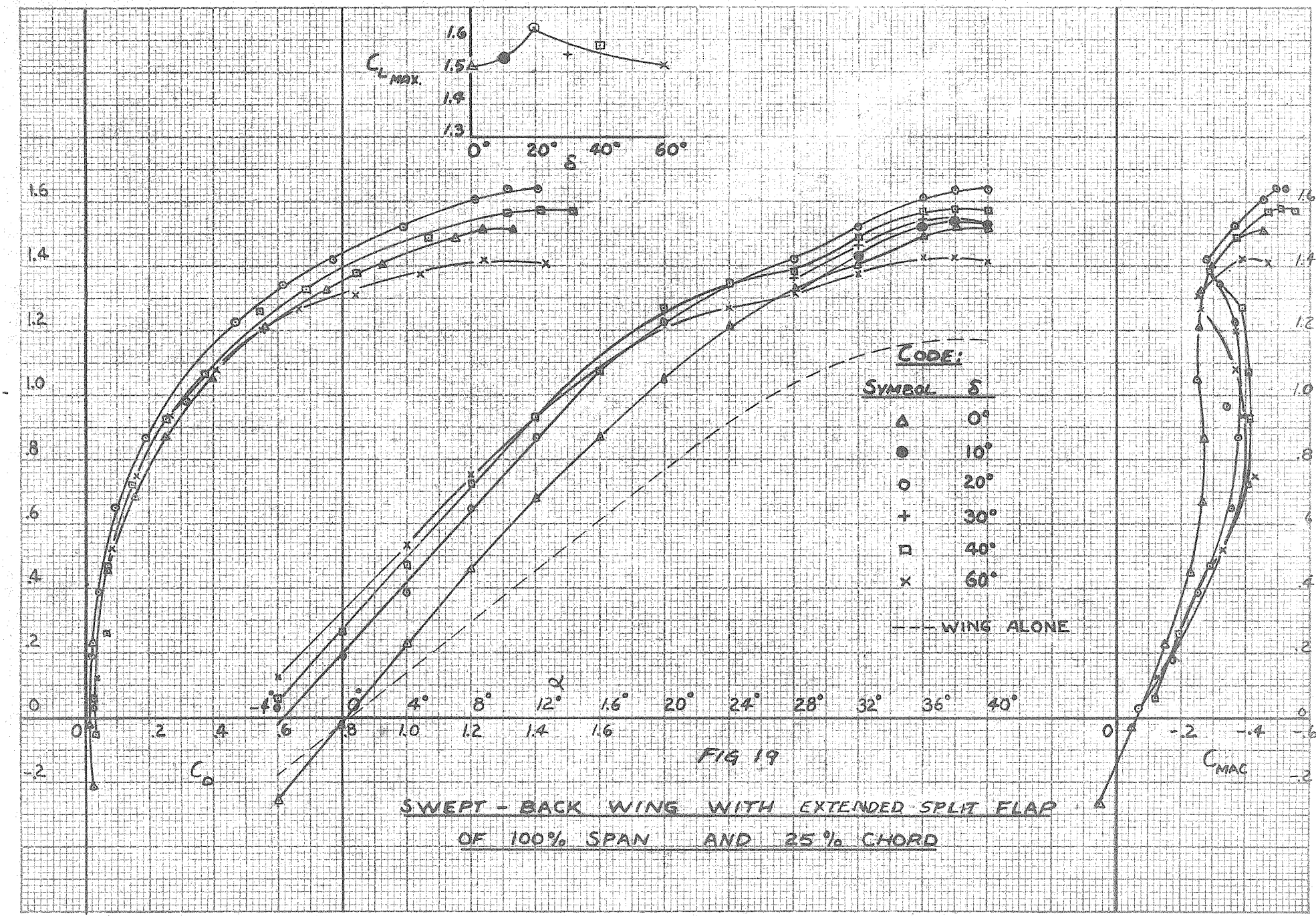

FIG 19

SWEPT - BACK WING WITH EXTENDED SPLIT FLAP OF 100% SPAN AND 25% CHORD

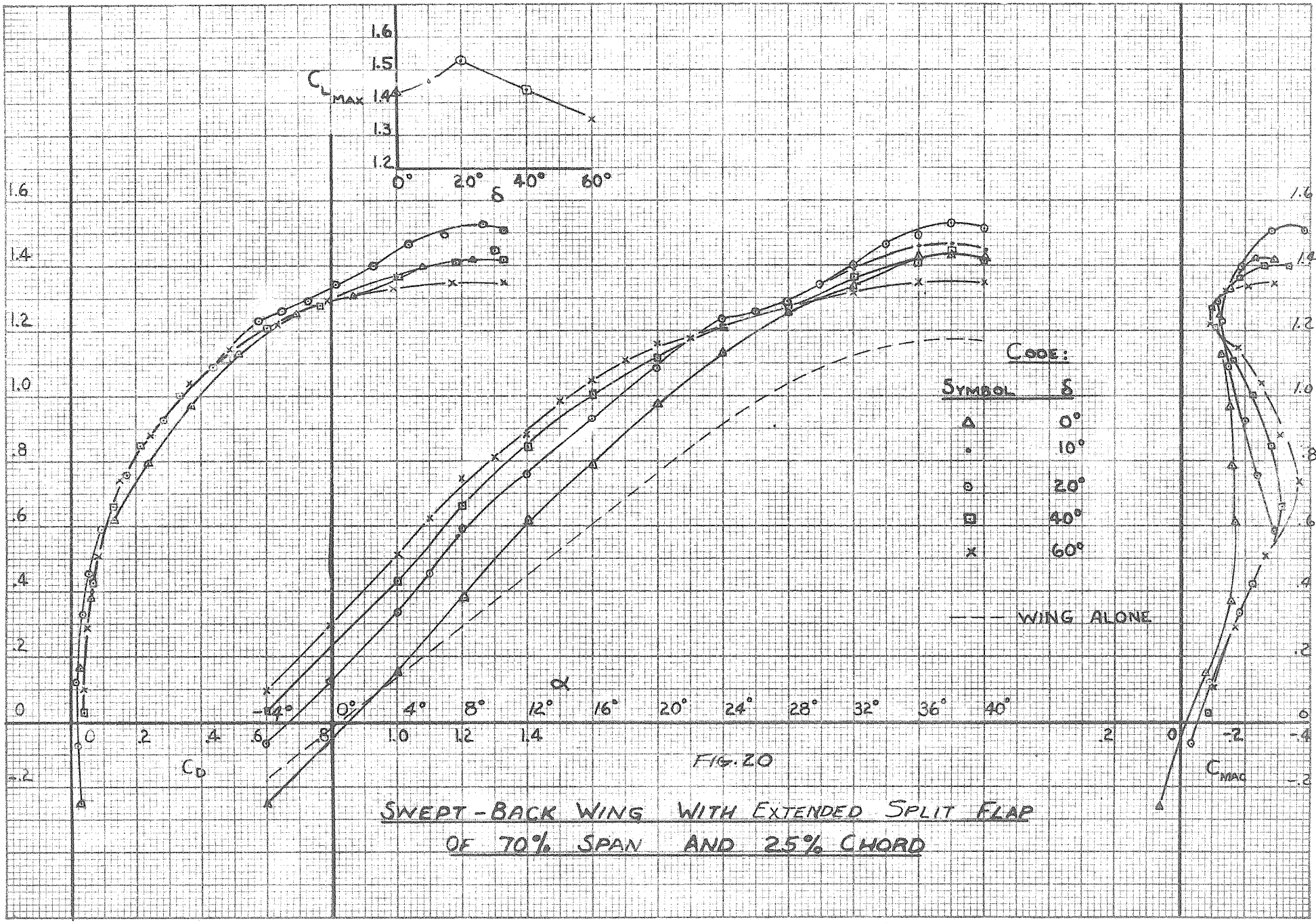

FIG. 20

SWEPT-BACK WING WITH EXTENDED SPLIT FLAP OF 70% SPAN AND 25% CHORD

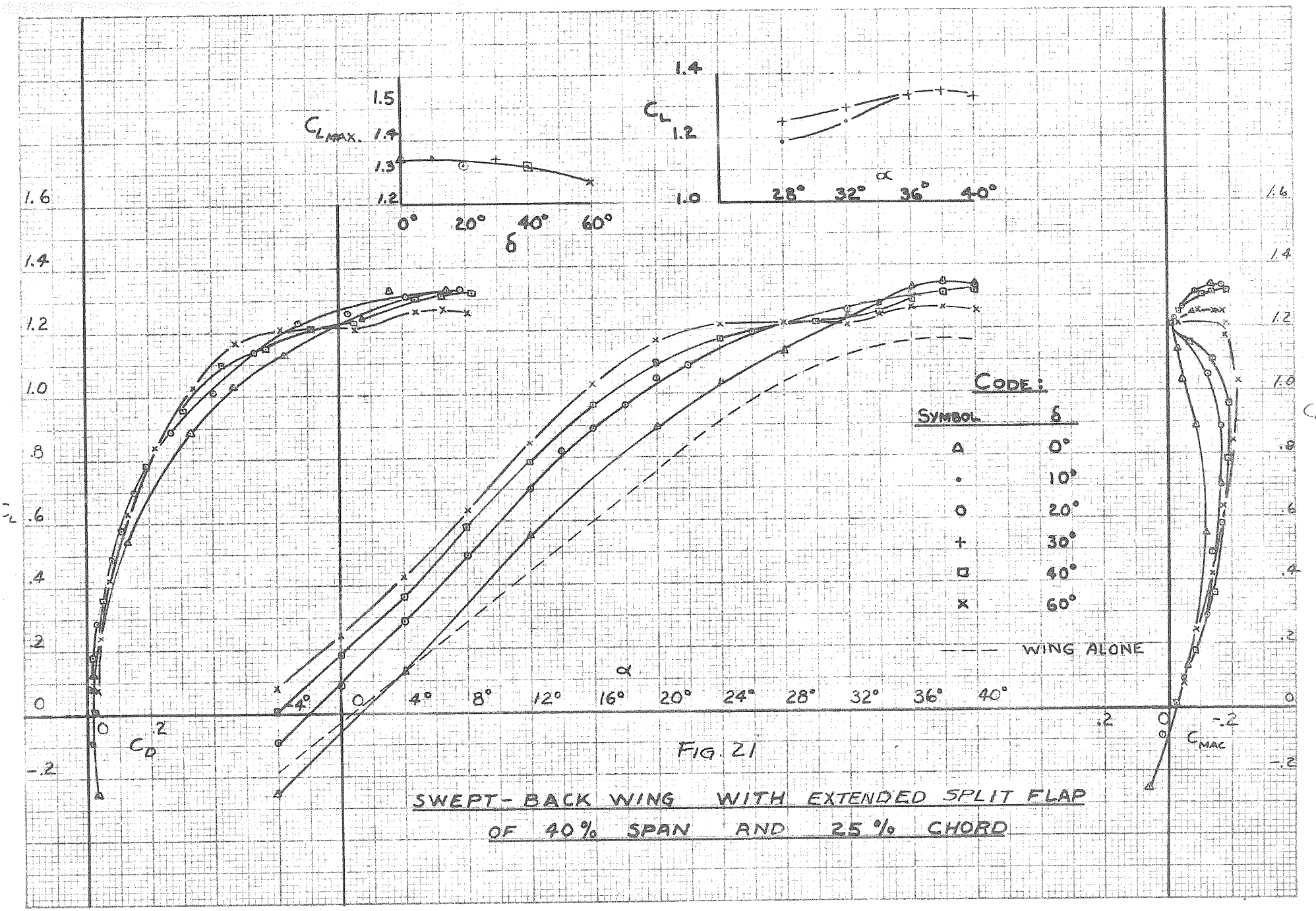

FIG. 21

SWEPT-BACK WING WITH EXTENDED SPLIT FLAP OF 40% SPAN AND 25% CHORD

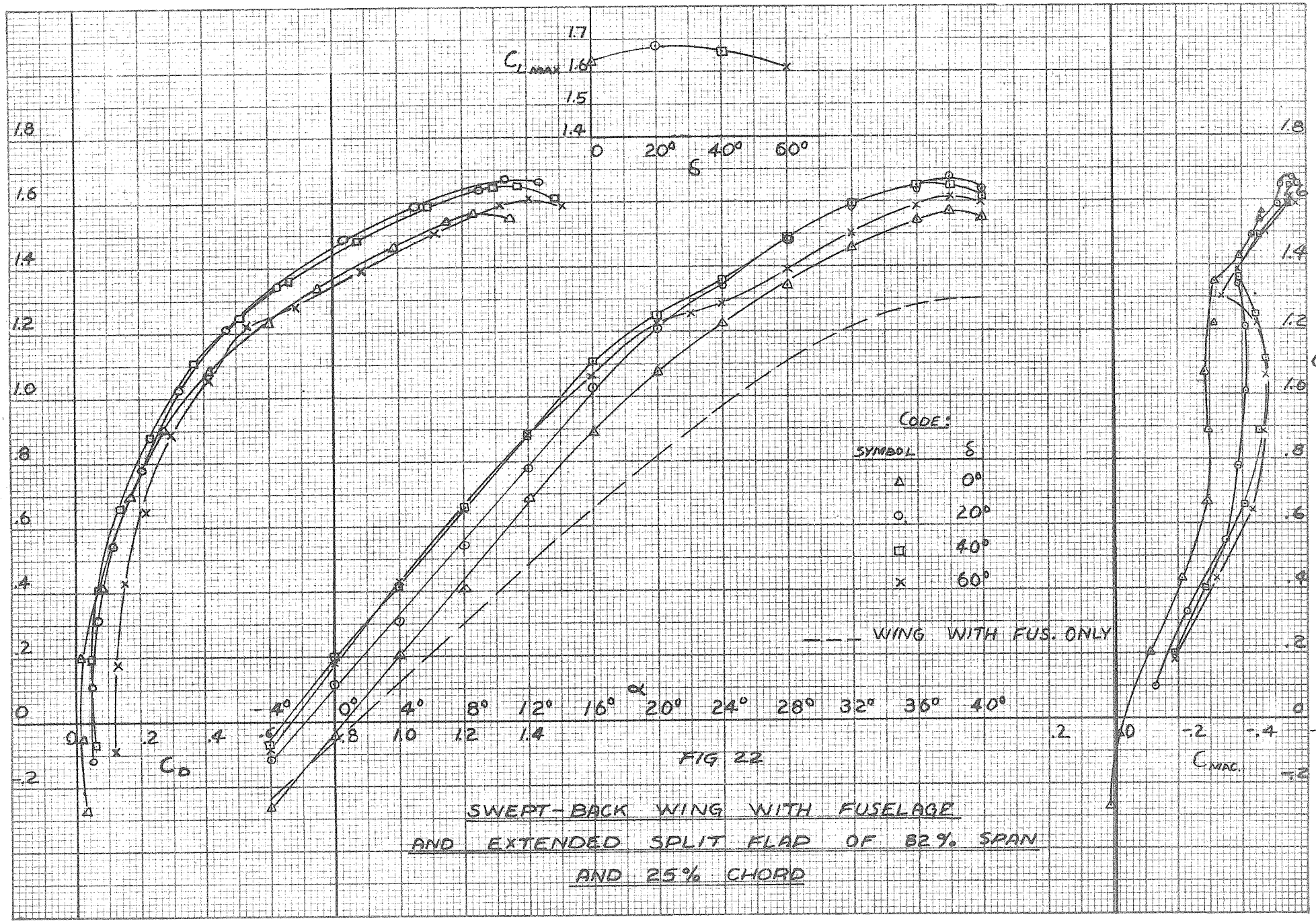

FIG 22

SWEPT-BACK WING WITH FUSELAGE AND EXTENDED SPLIT FLAP OF 82% SPAN AND 25% CHORD

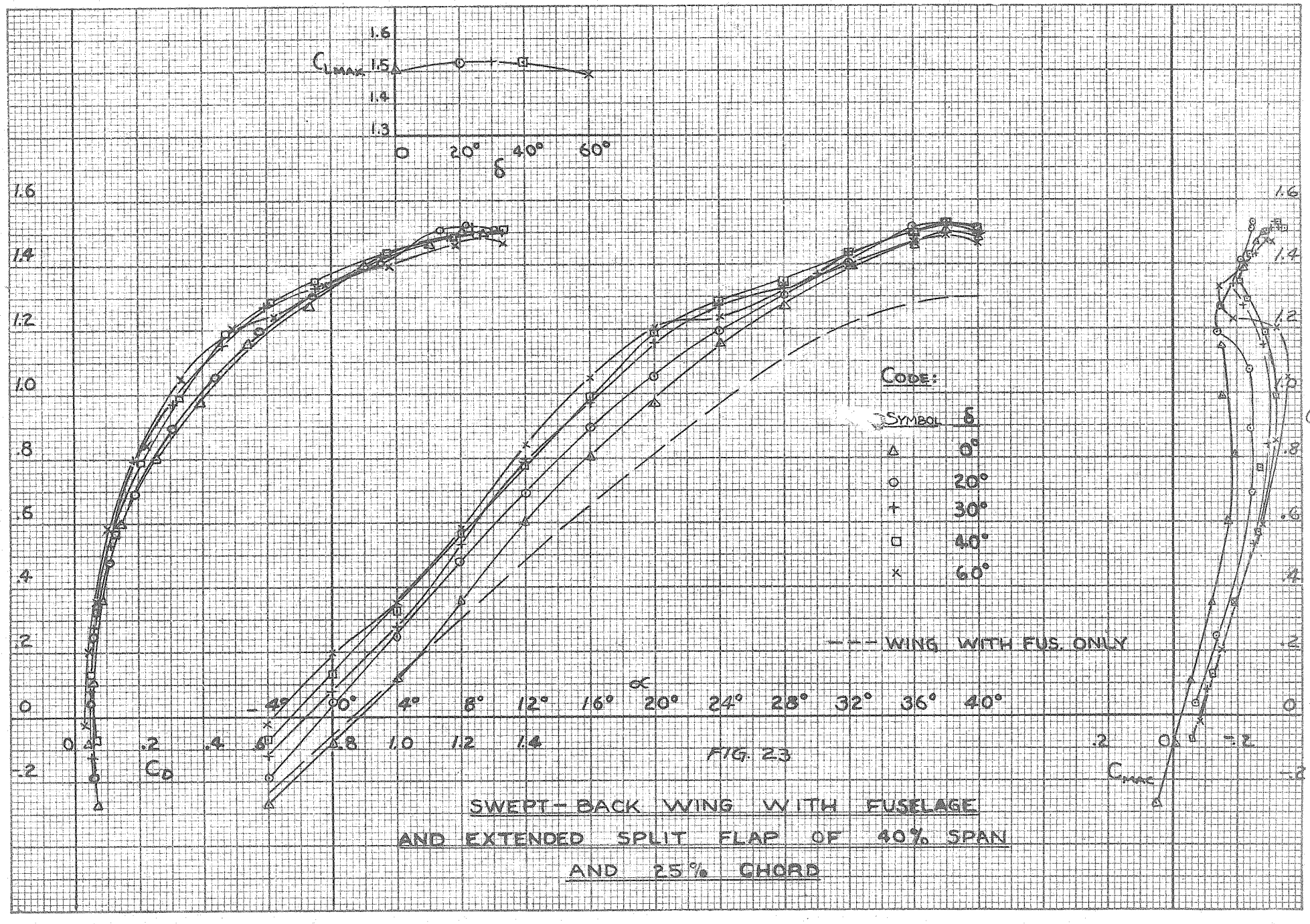

FIG. 23

SWEPT-BACK WING WITH FUSELAGE AND EXTENDED SPLIT FLAP OF 40% SPAN AND 25% CHORD

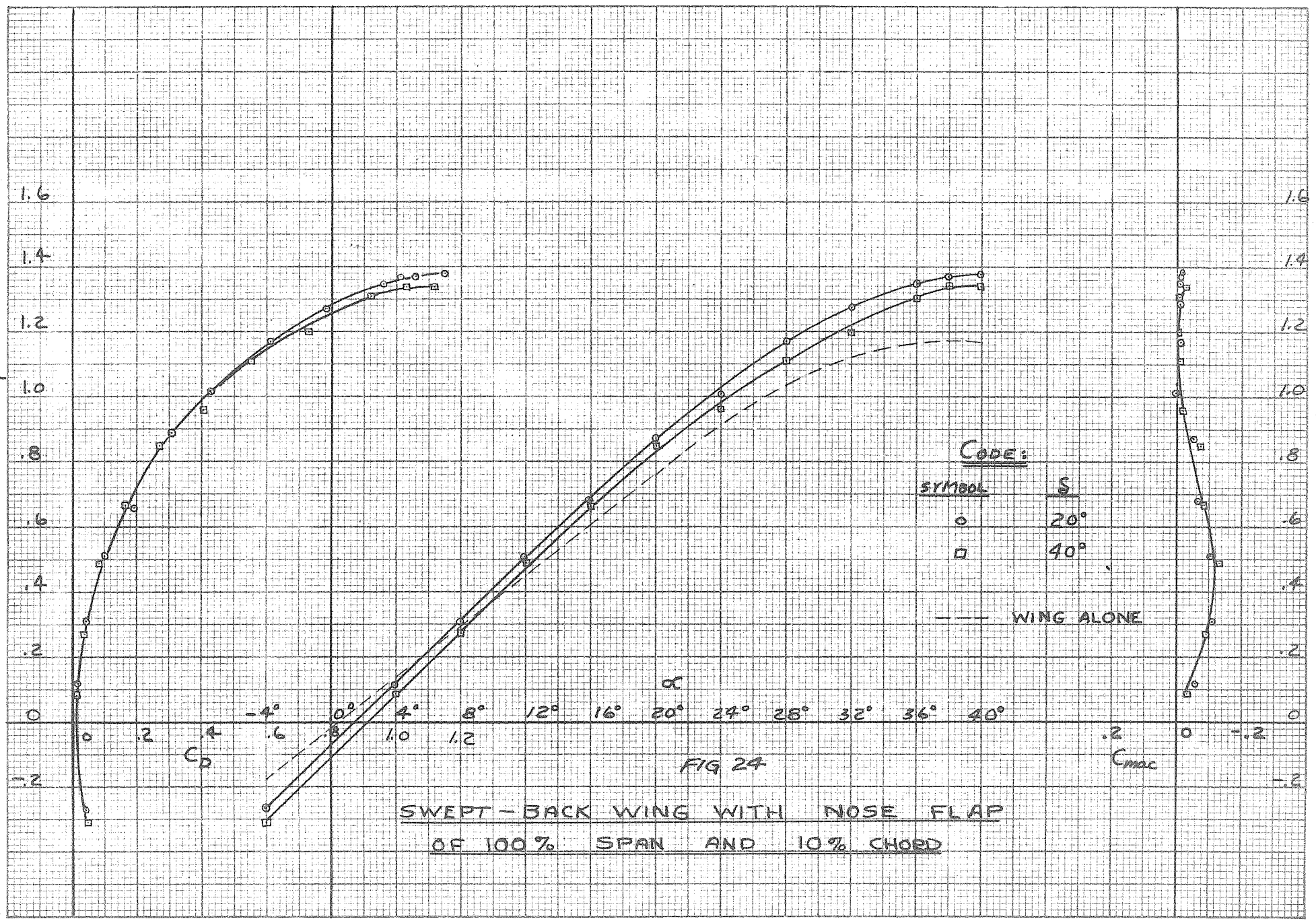

FIG 24

SWEPT-BACK WING WITH NOSE FLAP OF 100% SPAN AND 10% CHORD

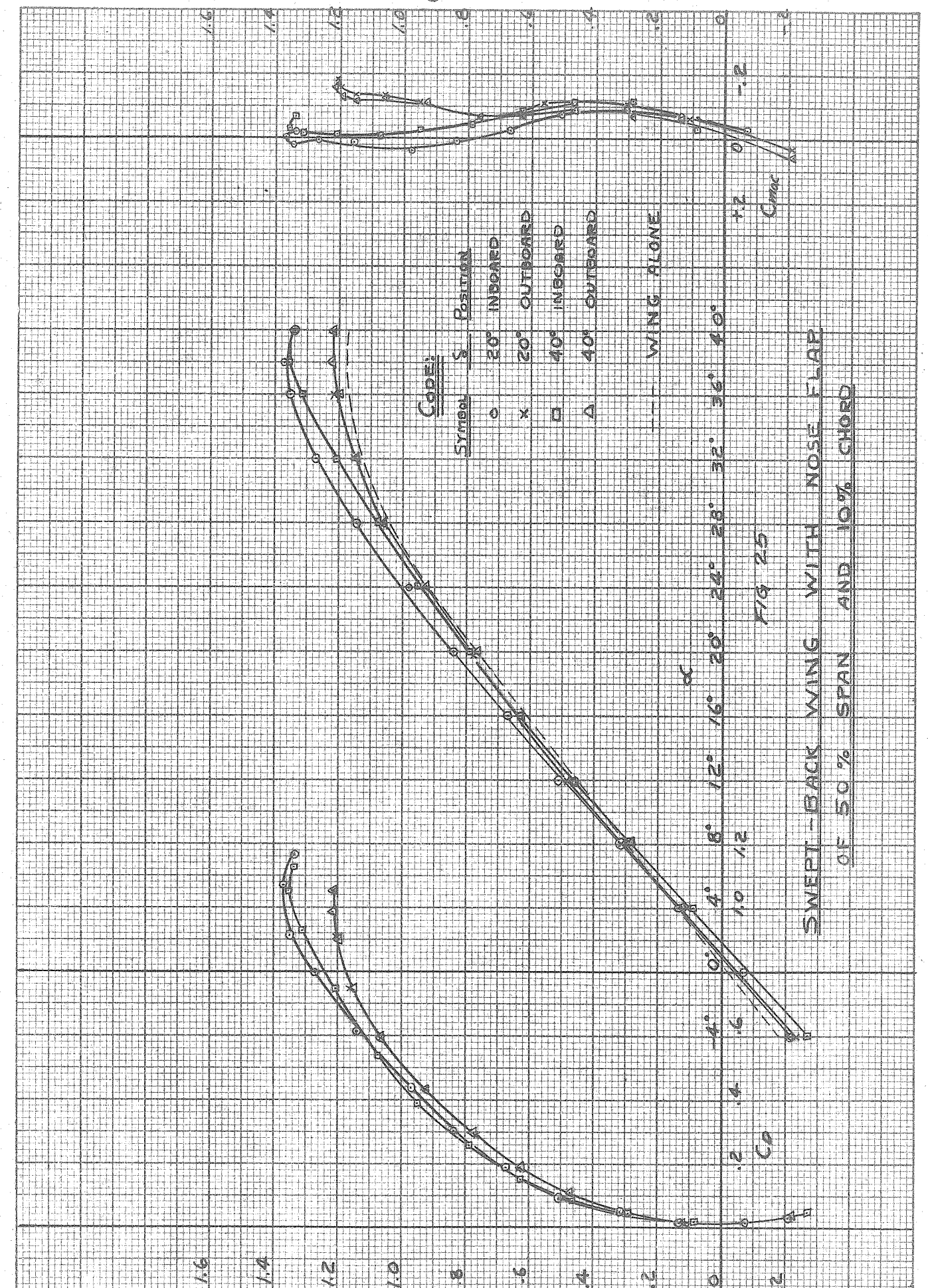
SWEPT-BACK WING WITH NOSE FLAP
OF 50% SPAN AND 10% CHORD
FIG 25
CODE:
Symbol δ Position
○ 20° INBOARD
× 20° OUTBOARD
□ 40° INBOARD
△ 40° OUTBOARD
— — WING ALONE
α
-4° 0° 4° 8° 12° 16° 20° 24° 28° 32° 36° 40°
Cmac
CL
CD

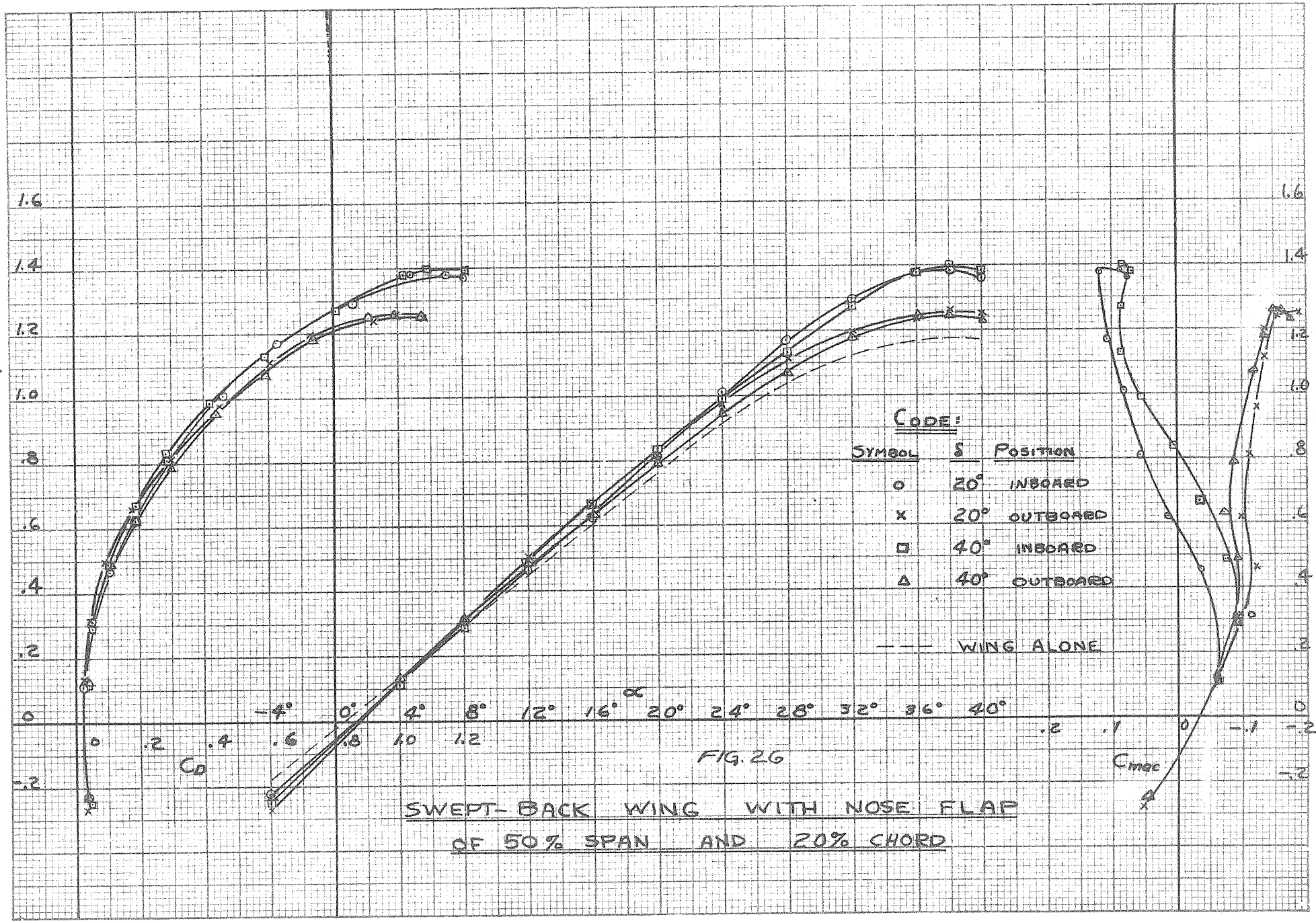

FIG. 26

SWEPT-BACK WING WITH NOSE FLAP
OF 50% SPAN AND 20% CHORD

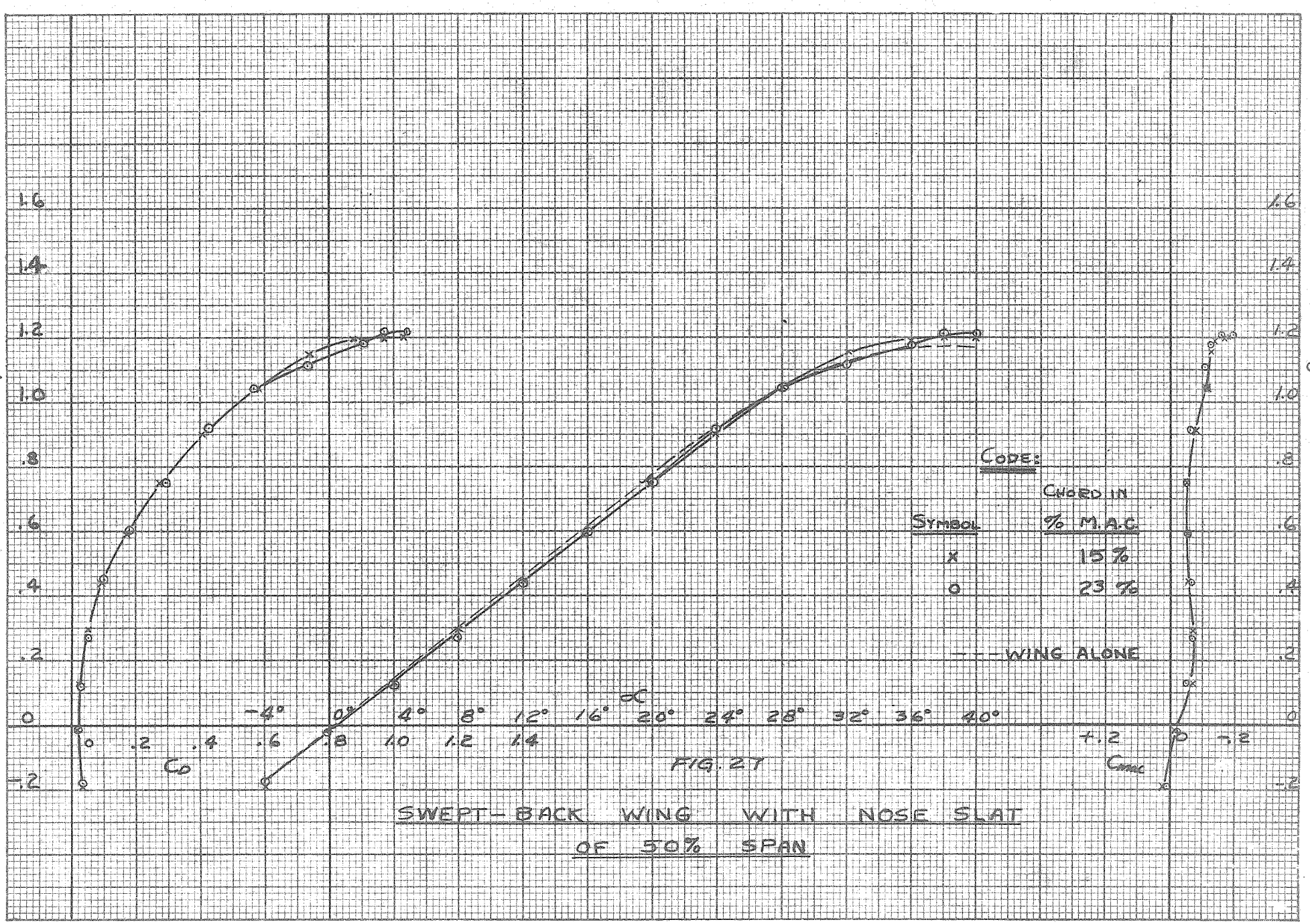

FIG. 27

SWEPT-BACK WING WITH NOSE SLAT OF 50% SPAN

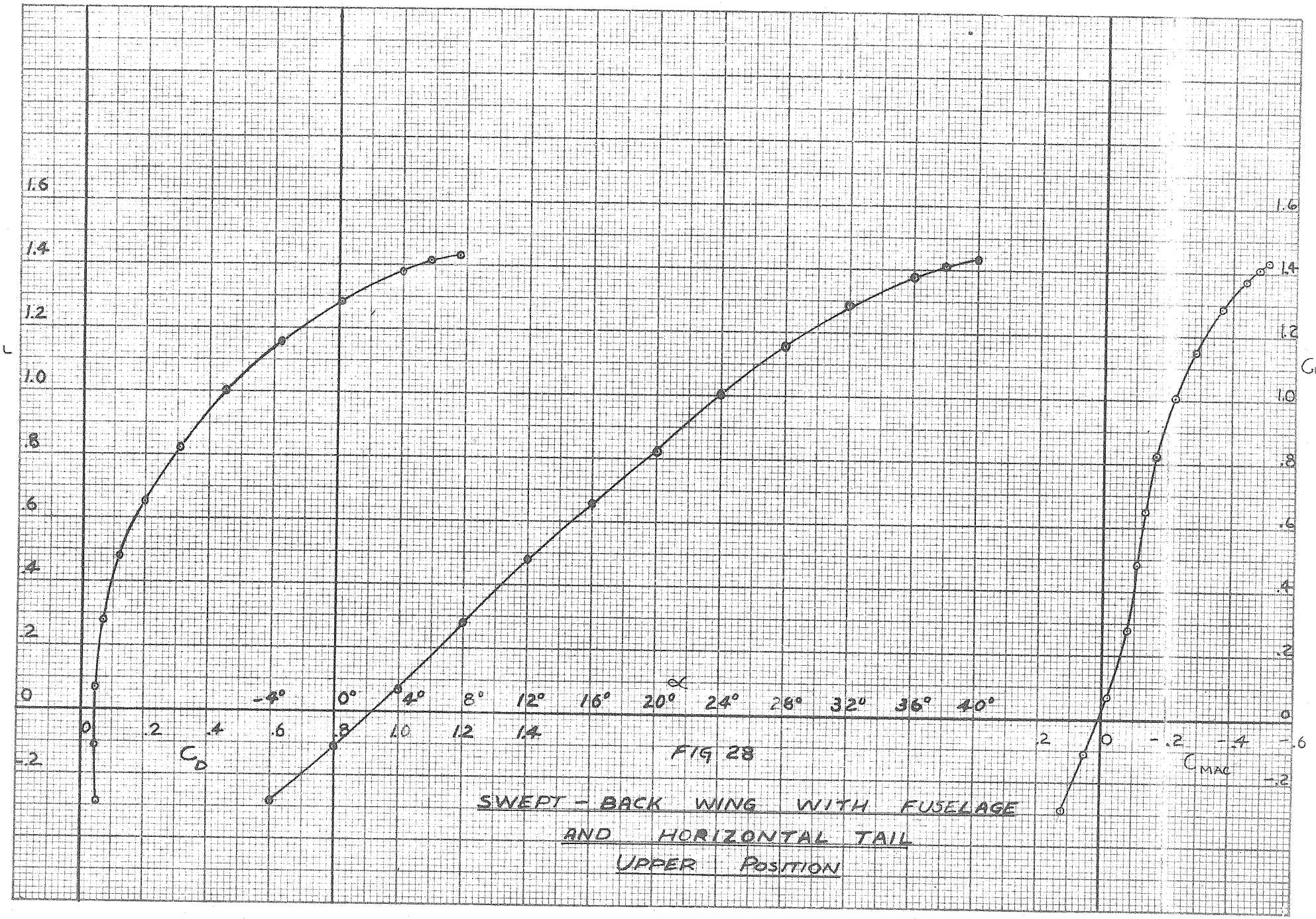

FIG 28

SWEPT - BACK WING WITH FUSELAGE AND HORIZONTAL TAIL UPPER POSITION

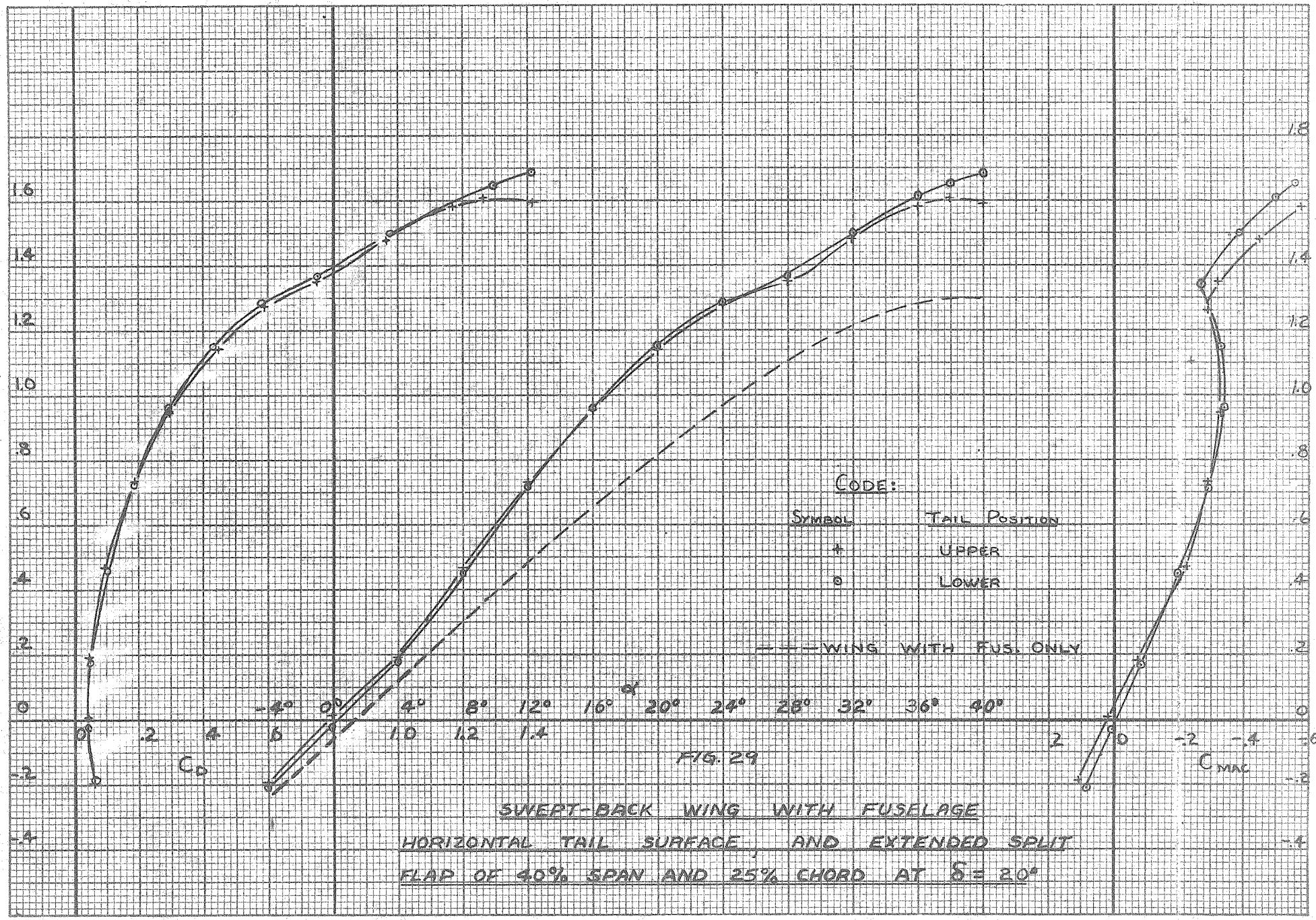

FIG. 29

SWEPT-BACK WING WITH FUSELAGE, HORIZONTAL TAIL SURFACE, AND EXTENDED SPLIT FLAP OF 40% SPAN AND 25% CHORD AT $\delta = 20°$

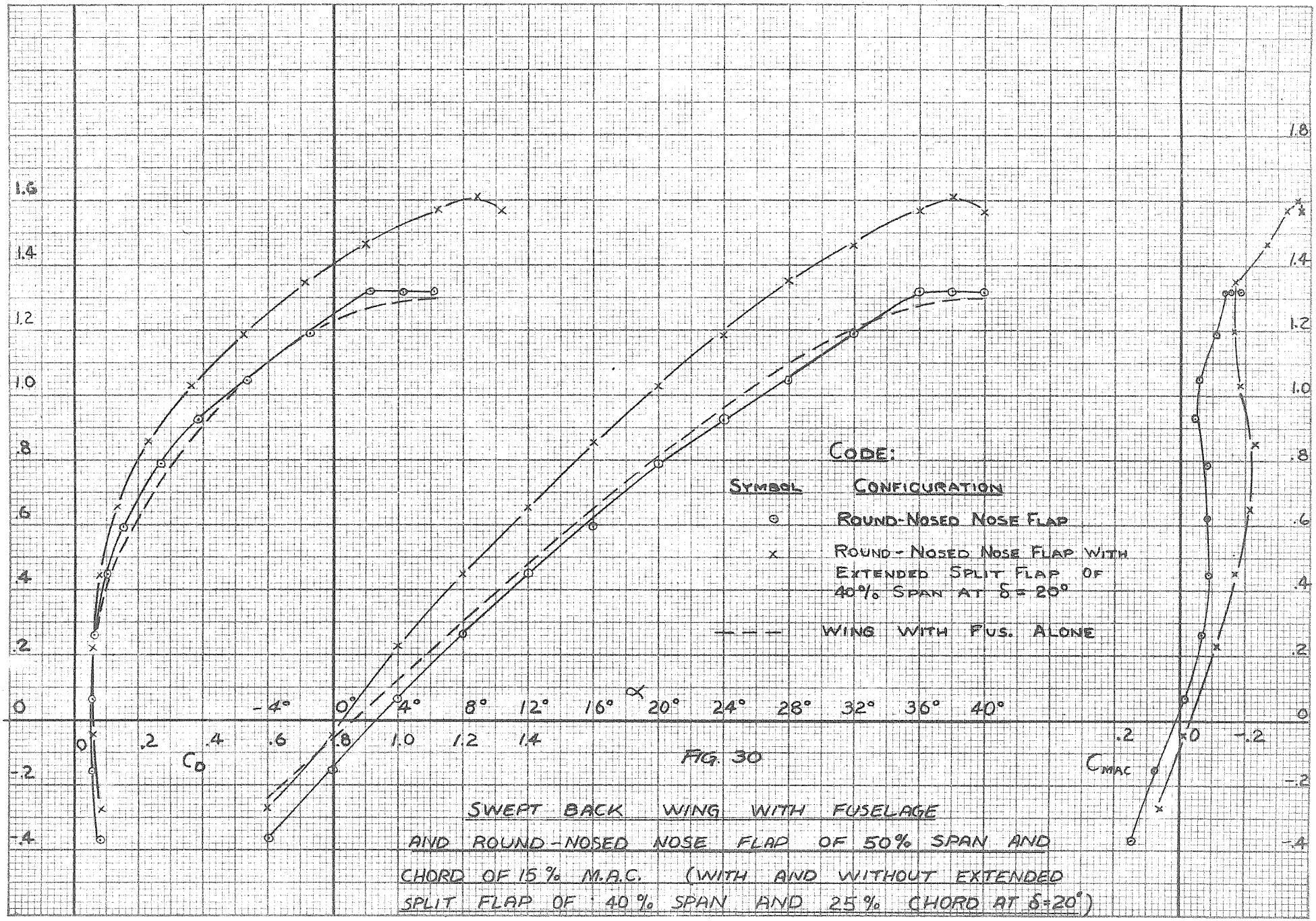

FIG. 30

SWEPT BACK WING WITH FUSELAGE AND ROUND-NOSED NOSE FLAP OF 50% SPAN AND CHORD OF 15% M.A.C. (WITH AND WITHOUT EXTENDED SPLIT FLAP OF 40% SPAN AND 25% CHORD AT δ=20°)

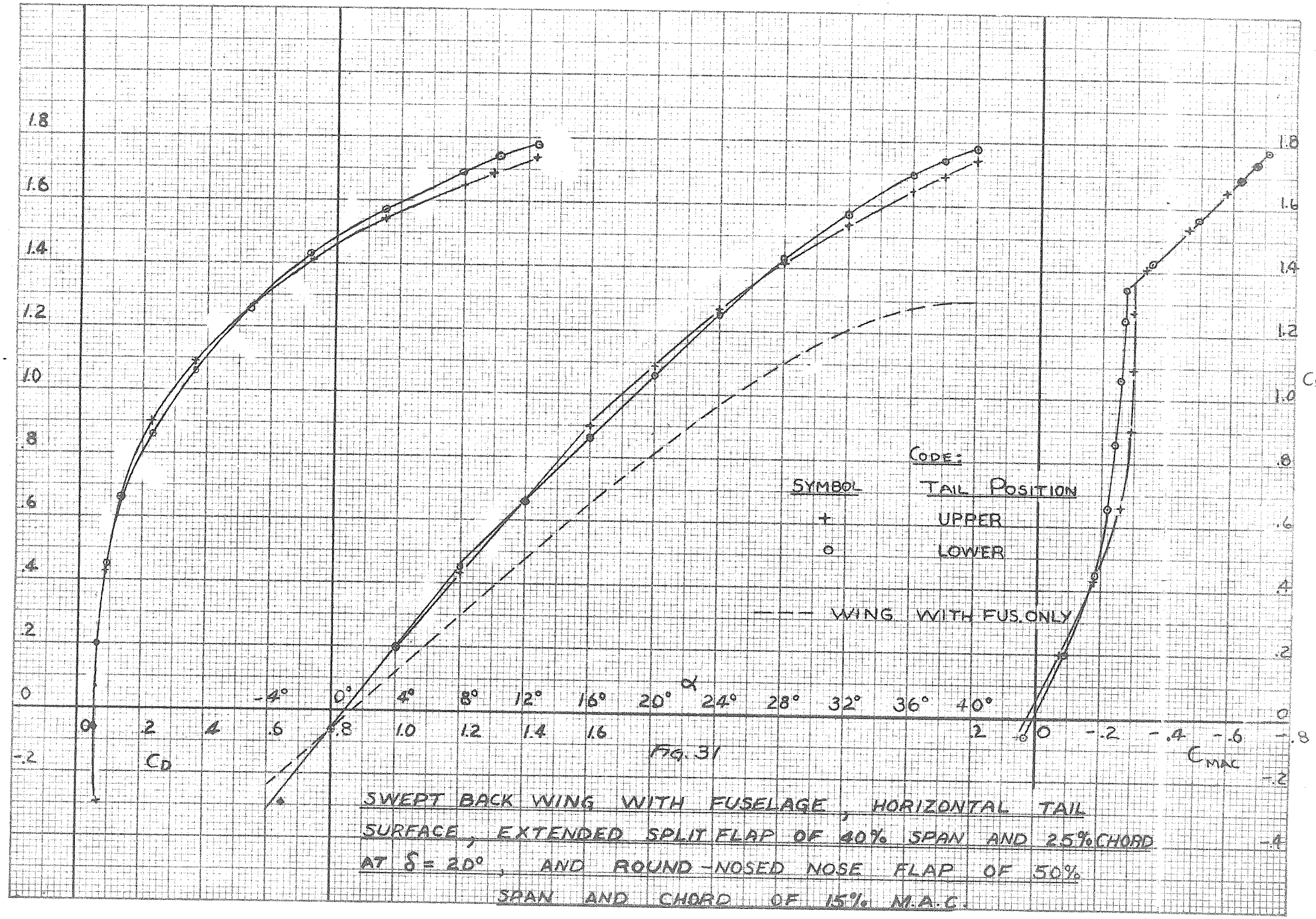

Fig. 31

SWEPT BACK WING WITH FUSELAGE, HORIZONTAL TAIL SURFACE, EXTENDED SPLIT FLAP OF 40% SPAN AND 25% CHORD AT $\delta = 20°$, AND ROUND-NOSED NOSE FLAP OF 50% SPAN AND CHORD OF 15% M.A.C.

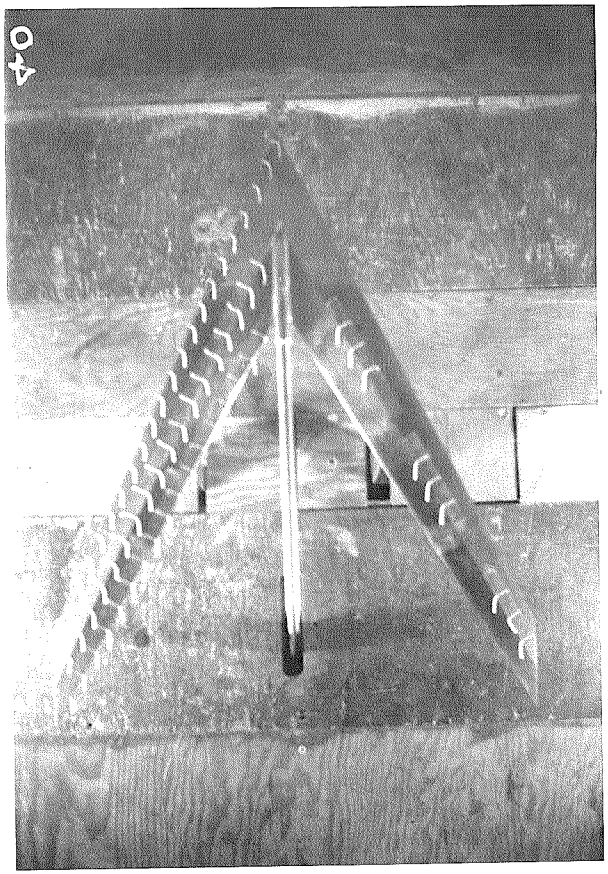

$\alpha = 0°$

Fig. 32

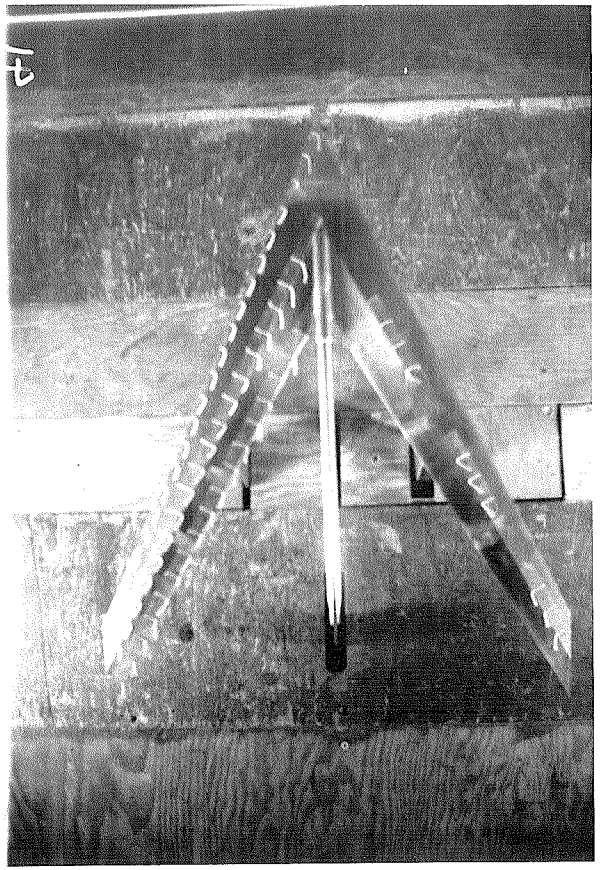

$\alpha = 8°$

Fig. 33

Tuft Studies of Wing With 70% Span

Split Flap Deflected 20°

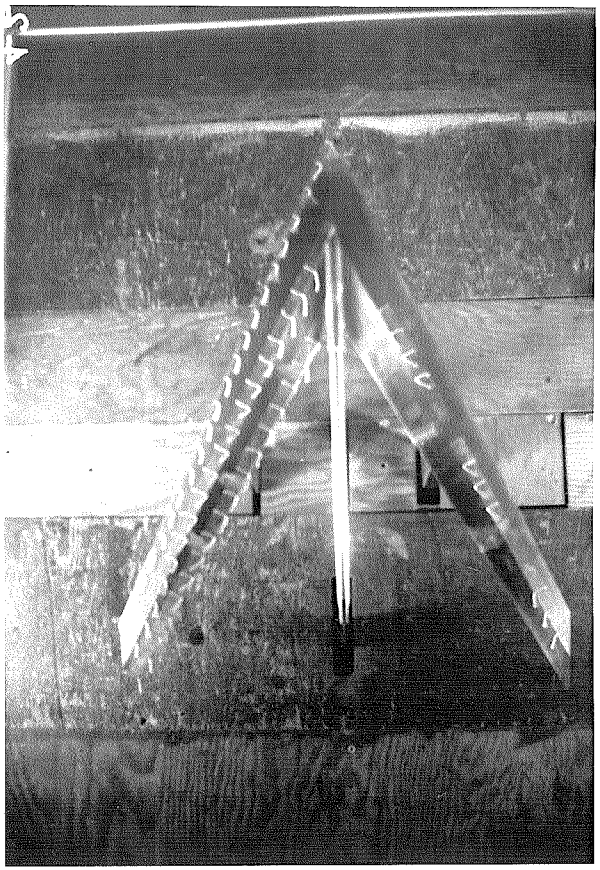

$\alpha = 12°$

Fig. 34

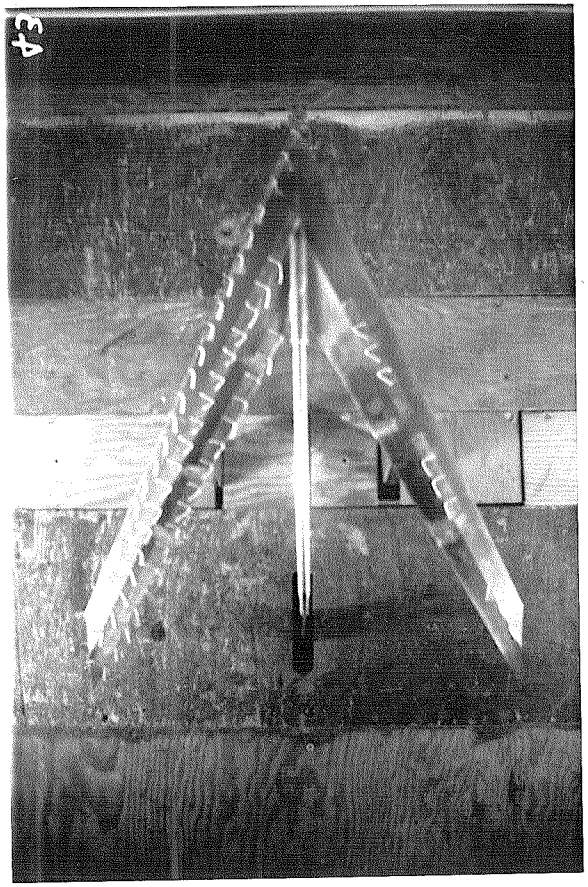

$\alpha = 16°$

Fig. 35

Tuft Studies of Wing With 70% Span

Split Flap Deflected 20°

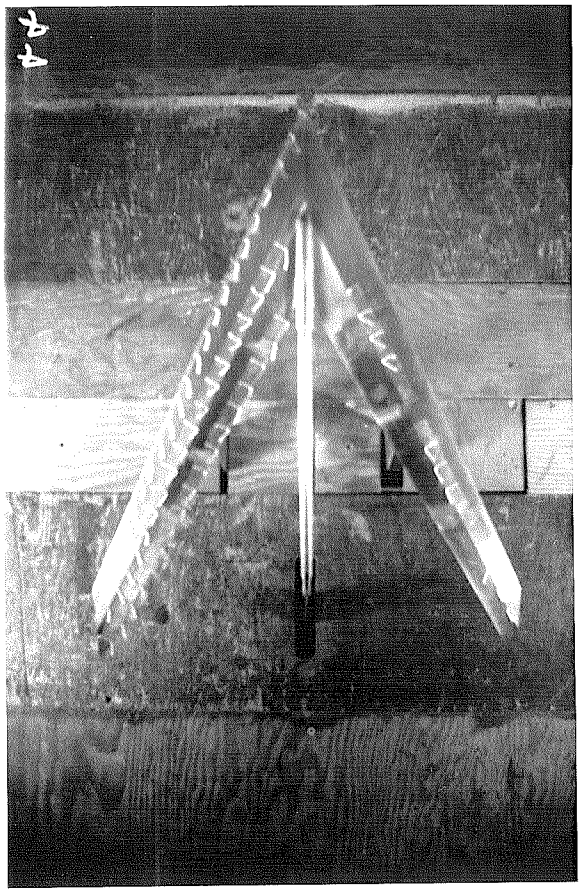

$\alpha = 20°$

Fig. 36

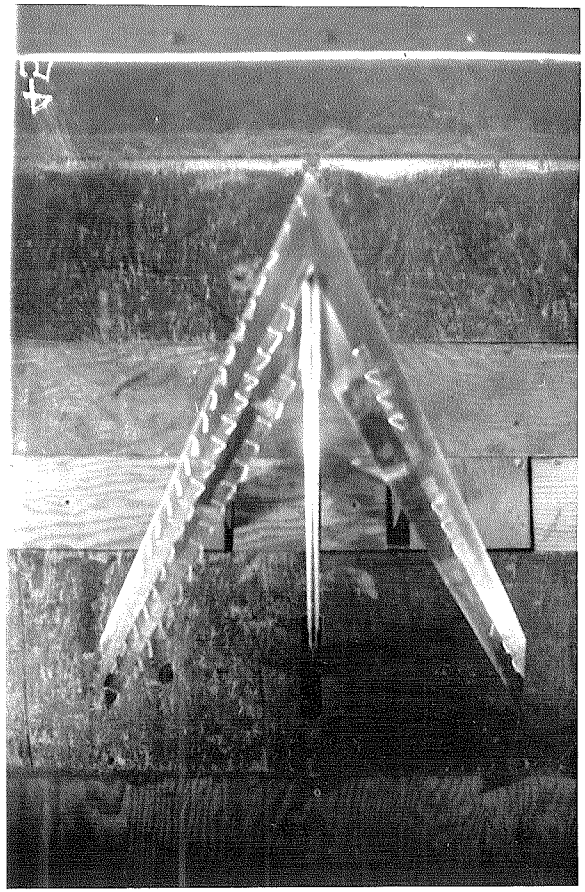

$\alpha = 24°$

Fig. 37

Tuft Studies of Wing With 70% Span

Split Flap Deflected 20°

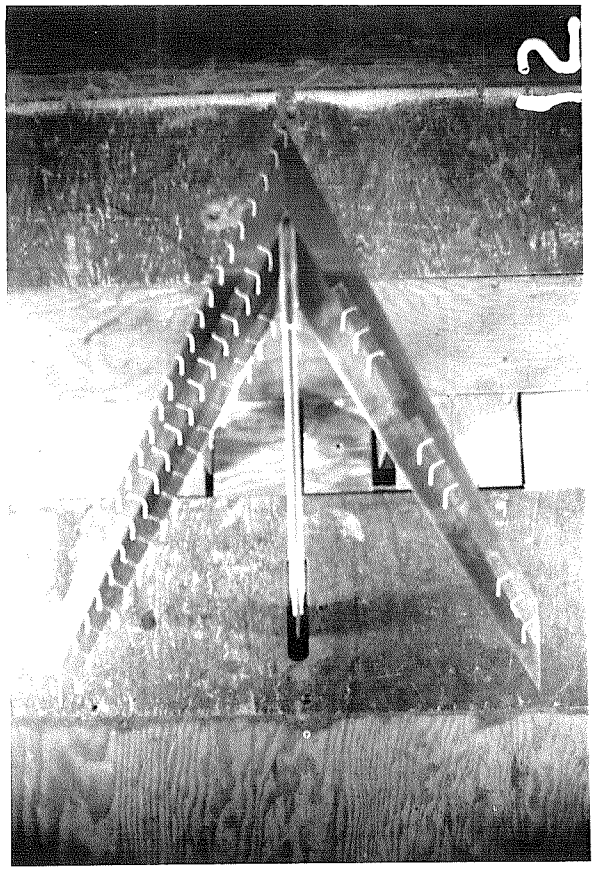

$\alpha = 0°$

Fig. 38

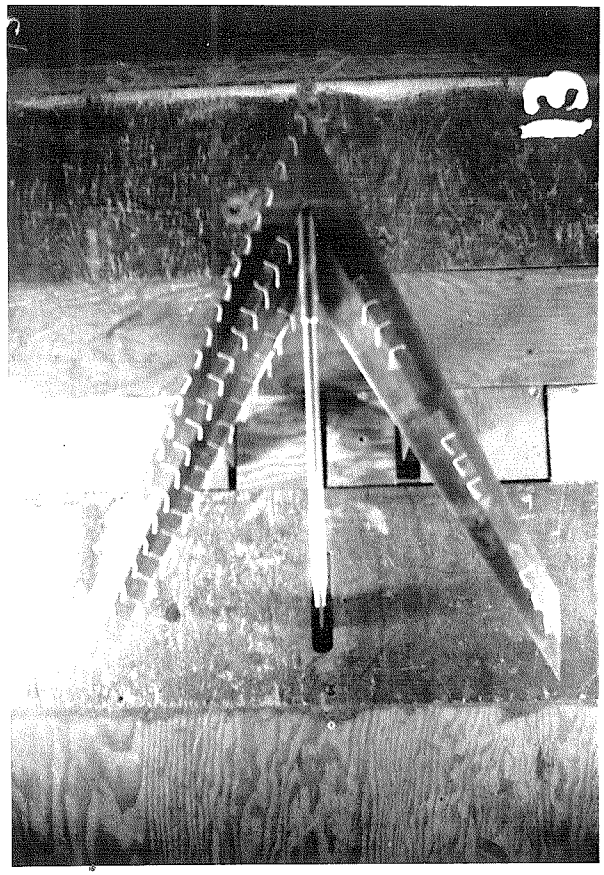

$\alpha = 4°$

Fig. 39

Tuft Studies of Wing Alone

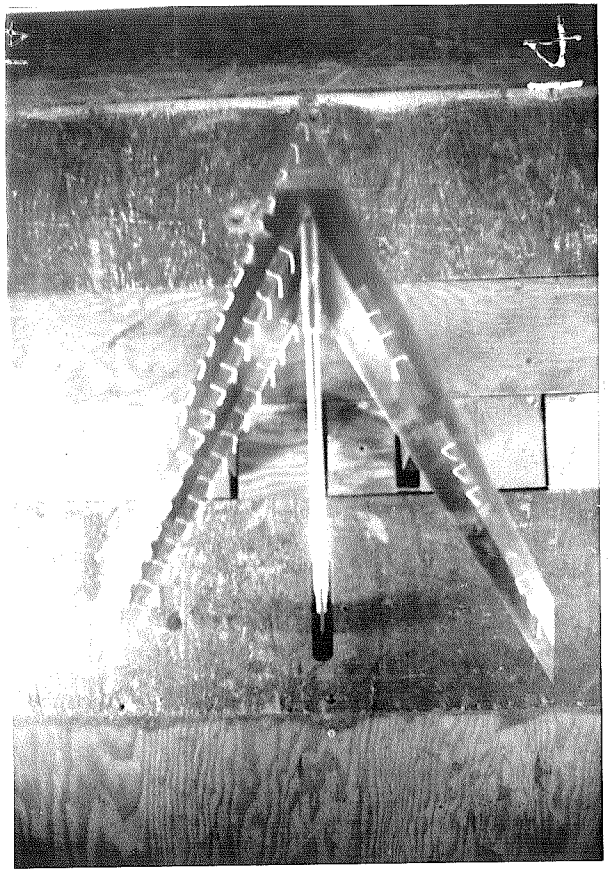

$\alpha = 8°$

Fig. 40

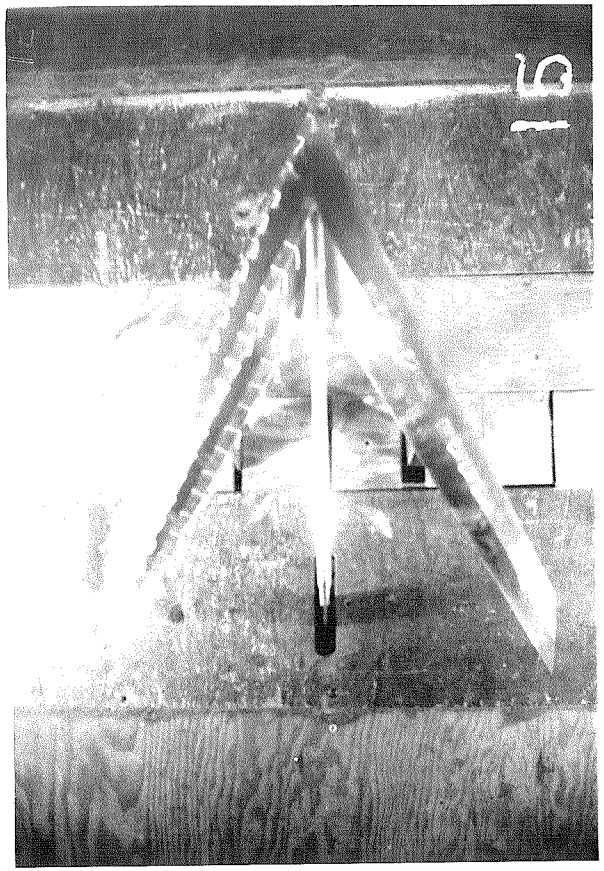

$\alpha = 12°$

Fig. 41

Tuft Studies of Wing Alone

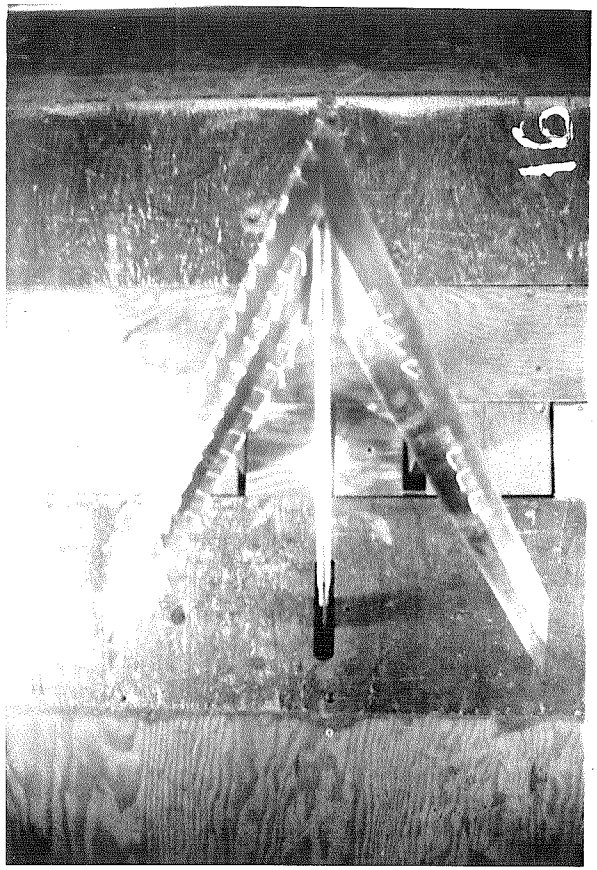

$\alpha = 16°$

Fig. 42

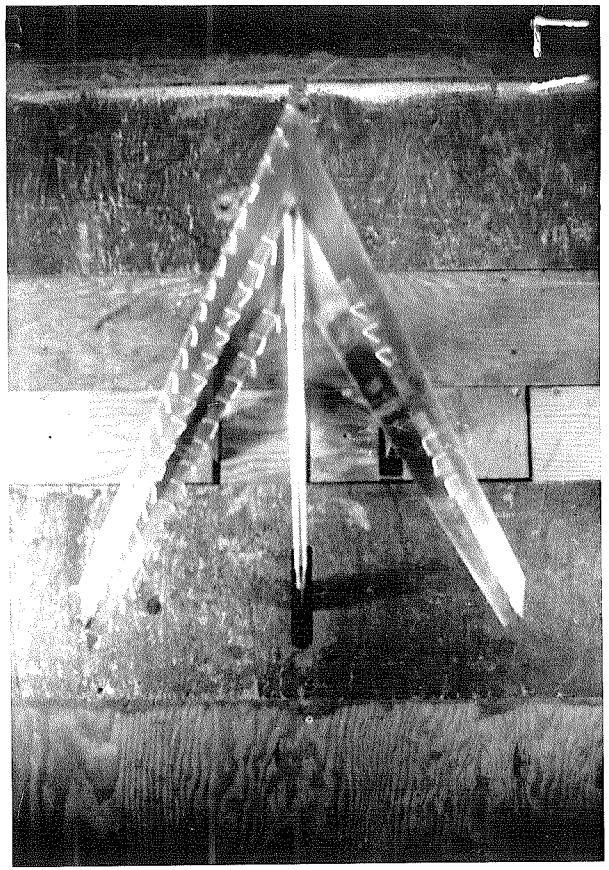

$\alpha = 20°$

Fig. 43

Tuft Studies of Wing Alone

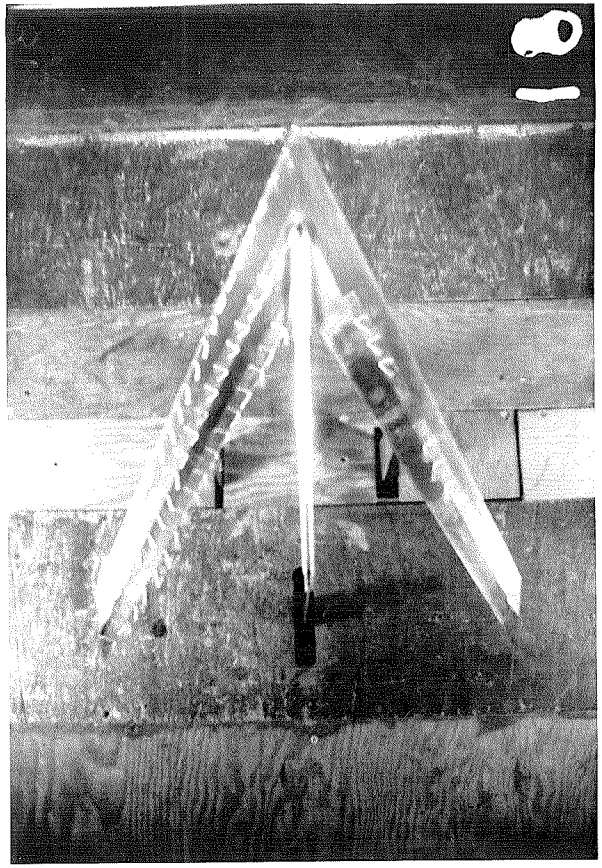

$\alpha = 24°$

Fig. 44

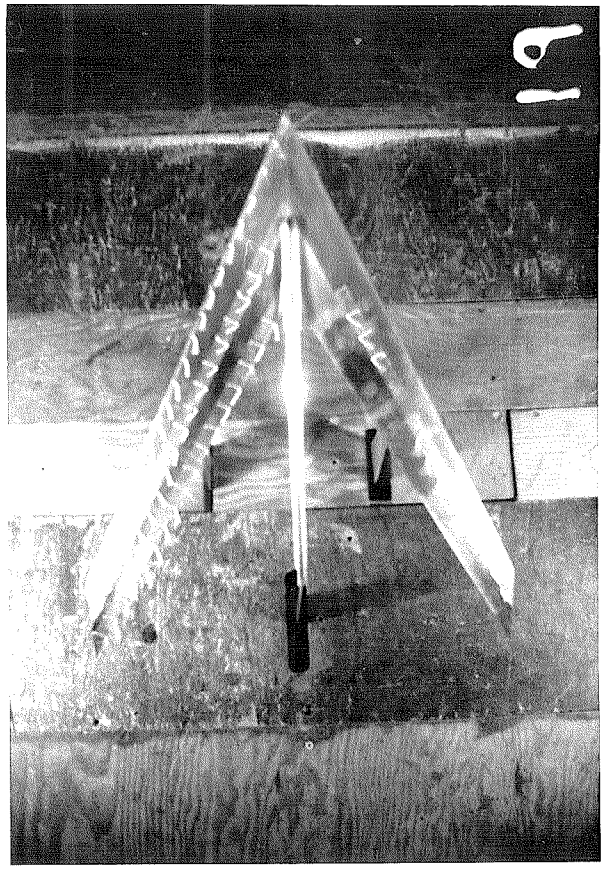

$\alpha = 28°$

Fig. 45

Tuft Studies of Wing Alone

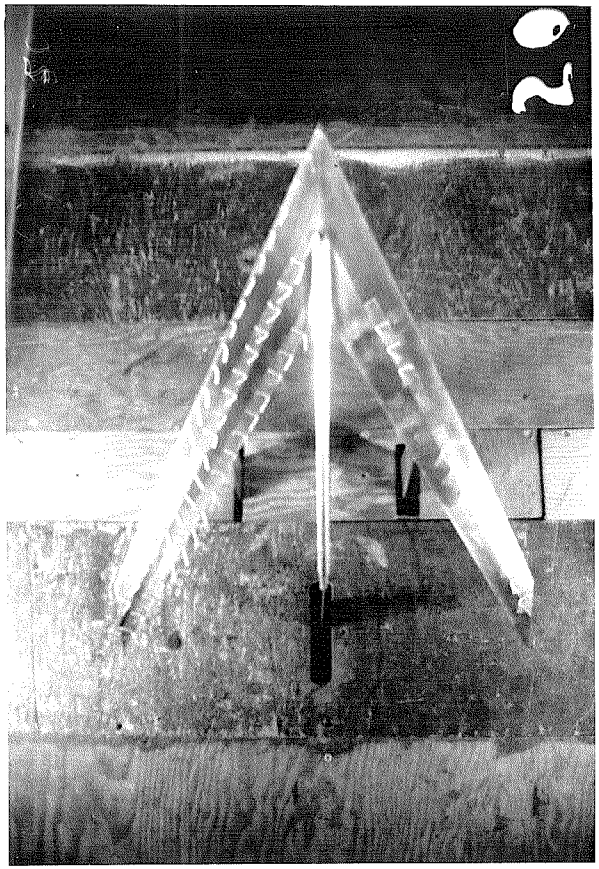

$\alpha = 32°$

Fig. 46

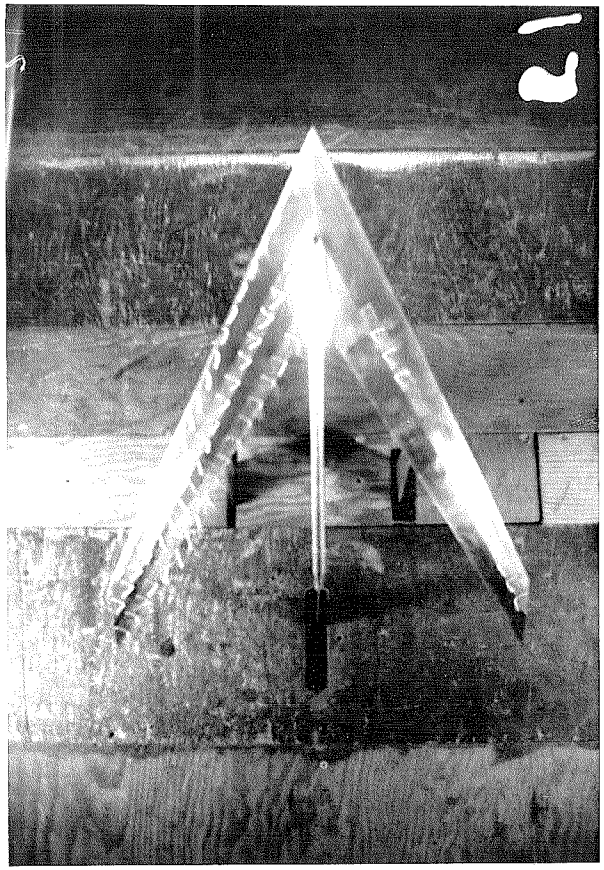

$\alpha = 36°$

Fig. 47

Tuft Studies of Wing Alone

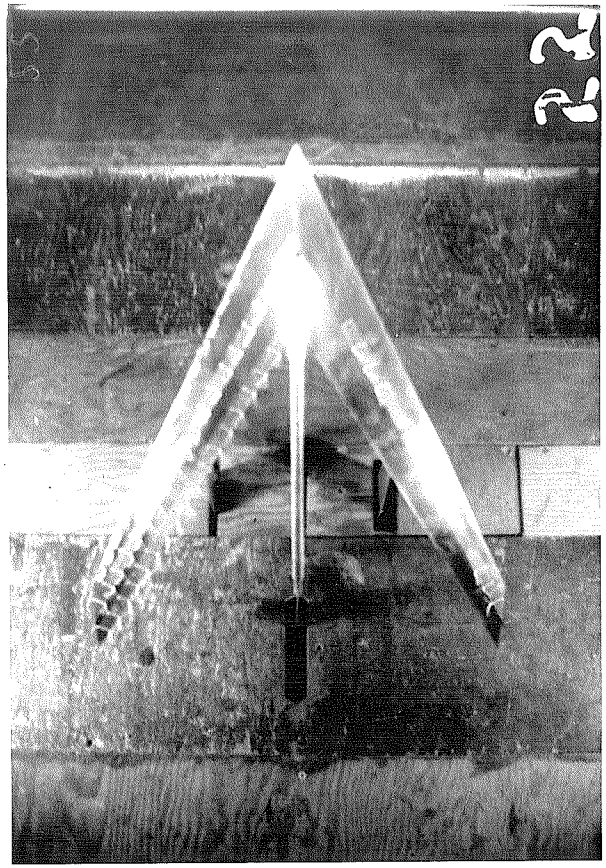

$\alpha = 40°$

Fig. 48

Tuft Studies of Wing Alone